Axion Dark Matter Search with Laser Interferometry

Yuta Michimura
Department of Physics, University of Tokyo

Contents

- Motivations
  - QCD axions
  - axion-like particles
- Searches for axion-photon coupling
  - review based on [PPNP **102**, 89 (2018)]
  - laboratory searches
  - helioscopes, haloscopes
  - astrophysical observations
- Interferometric search
  - review of proposals
  - possible prototype experiment
- Summary

Axion

- Hypothetical particle predicted by Peccei-Quinn mechanism to solve strong CP problem (QCD axion)
- Axion-like particles (ALPs)
  - string theories
  - inflation models　etc……
- Also leading candidates of cold dark matter

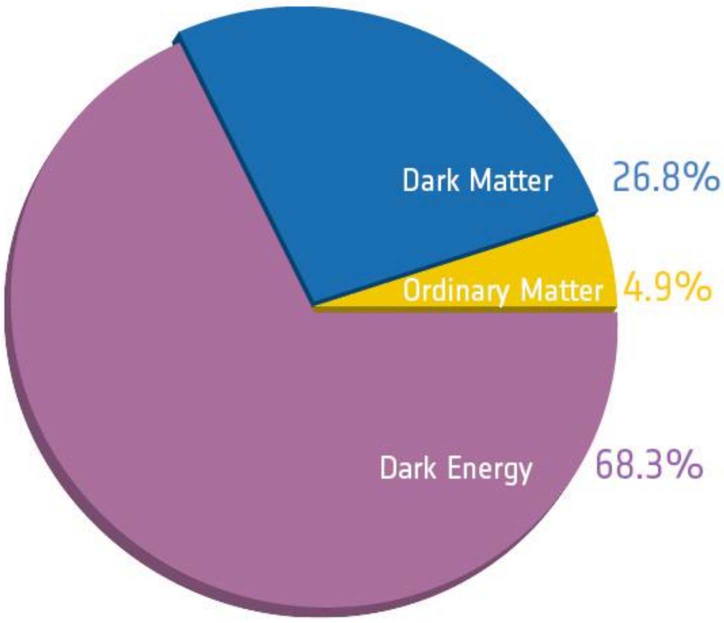

Strong CP Problem

- QCD allows CP violation

gluon field strength tensor

$$\mathcal{L}_{\rm QCD} = \mathcal{L}_0 + \frac{\theta_{\rm QCD}}{32\pi} G_{\mu\nu}\tilde{G}^{\mu\nu}$$

- CP violation in strong interactions never found
- Neutron electric dipole moment measured to be

$$d_{\rm n} < 3.0 \times 10^{-13} e\,{\rm fm}$$ PRL **97**, 131801 (2006)

this means

$$|\theta_{\rm QCD}| < 1.3 \times 10^{-10}$$

(fine tuning problem; $0 < \theta_{\rm QCD} < 2\pi$)

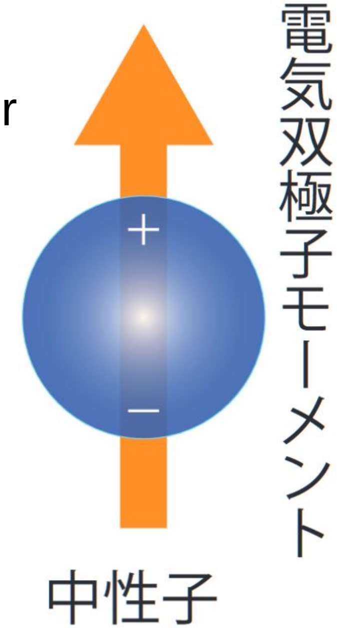

http://www.icrr.u-tokyo.ac.jp/ICRR_news/ICRRnews37.pdf

- Peccei-Quinn theory
  - introduce a scalar field with $\mathrm{U(1)_{PQ}}$ symmetry

$$\Psi_{\rm PQ} = |\Psi_{\rm PQ}| e^{i\theta} \simeq f_A e^{i\frac{A}{f_A}}$$

axion field

axion decay constant

???

  - this symmetry is spontaneously broken at energy scale f_A
  - implies pseudo (has mass) Nambu-Goldstone boson: axion
  - minimum QCD vacuum energy at $\theta = 0$

QCD Axion Models

- How to break $U(1)_{PQ}$ symmetry
  - Weinberg-Wilczek model (two Higgs doublets)
    soon experimentally excluded
  - KSVZ model (heavy quark + a new scalar)
  - DFSZ model (two Higgs doublets + a SM singlet scalar)
    invisible axion models

- QCD axion do not have a mass in the early universe, but gets mass after a QCD phase transition via instanton effect

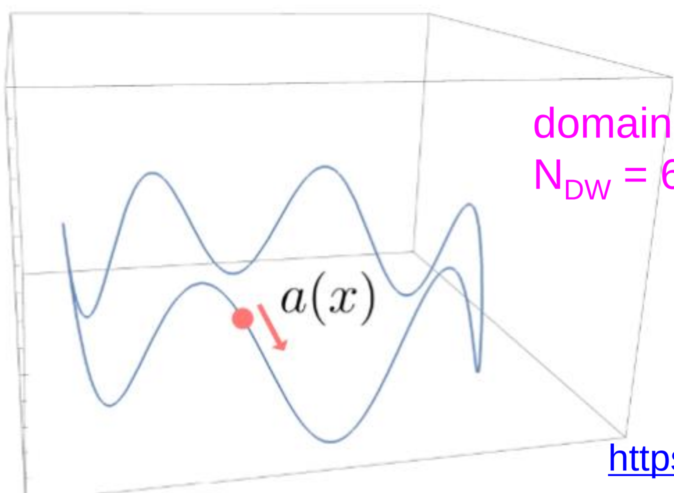

domain wall number
N_{DW} = 6 case

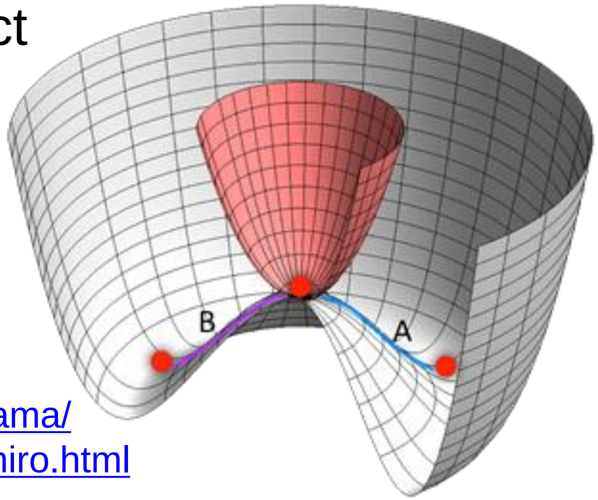

http://research.kek.jp/people/hkodama/UTQuestHP/RHL_KawasakiMasahiro.html

https://conference-indico.kek.jp/indico/event/36/session/13/contribution/32/material/slides/0.pdf

QCD Axion Models

- There are many other models of QCD axion

Table 1
CP and flavour conserving QCD Axion couplings in selected models. Some ranges are limited by perturbativity of the Yukawa couplings. In hadronic models, fermion couplings arise at the loop level in the high-energy theory, while the low energy couplings to nucleons include meson mixing. A tilde indicates model variability uncertain to the authors (of this review).

Model	N_{DW}	High-E couplings				Low-E couplings			
		E/N	C_{Au}	C_{Ad}	C_{Ae}	$C_{A\gamma}$	C_{Ap}	C_{An}	C_{Ae}
PQWW	3	$8/3$	$c_\beta^2/3$	$s_\beta^2/3$	$s_\beta^2/3$	0.75	...	...	...
DFSZ I	6,3	$8/3$	$c_\beta^2/3$	$s_\beta^2/3$	$s_\beta^2/3$	0.75	(−0.2,-0.6)	(−0.16,0.26)	(0.024, 1/3)
DFSZ II	6,3	$2/3$	$c_\beta^2/3$	$s_\beta^2/3$	$-c_\beta^2/3$	−1.25	(−0.2,-0.6)	(−0.16,0.26)	(−1/3, 0)
KSVZ	1	0	g-loop	g-loop	0	−1.92	−0.47	−0.02(3)	$\sim 2\times10^{-4}$
Hadronic 1$\mathcal{Q}$ [86]	1...20	$1/6 \dots 44/3$	g-loop	g-loop	γ-loop	−0.25 ... 12.7[a]	−0.47	−0.02(3)	$(0.05 \dots 5)\times10^{-3}$
SMASH [16]	1	$8/3$, $2/3$	g-loop	g-loop	ν-loop	0.75,-1.25	−0.47	−0.02(3)	(−0.16, 0.16)
MFVA [94]	9	$2/3$, $8/3$	0	$1/3$	$1/3$	0.75, −1.25	~ -0.6	~ -0.26	$\sim 1/3$
Flaxion/Axi-flavon [11,12]	–	$8/3$	$\sim O(1)$	$\sim O(1)$	$\sim O(1)$	(0.5,1.1)	–	-	–
Astrophobic M1,2 [96]	1,2	$2/3$, $8/3$	$\sim 2/3$	$\sim 1/3$	~ 0	−1.25,0.75	$\sim 10^{-2}$	$\sim 10^{-2}$	~ 0
Astrophobic M3,4 [96]	1,2	$-4/3$, $14/3$	$\sim 2/3$	$\sim 1/3$	~ 0	−3.3,2.7	$\sim 10^{-2}$	$\sim 10^{-2}$	~ 0

[a] Only minimum and maximum values of E/N are quoted. For $C_{A\gamma}$'s, we quote the ones giving the minimum and maximum of its absolute value (the relevant for detection).

domain wall number

- Coupling constant and axion mass are related in QCD axions

$$g_{A\gamma} \equiv \frac{\alpha}{2\pi}\frac{C_{A\gamma}}{f_A} = 2.0\times10^{-16} C_{A\gamma}\frac{m_A}{\mu\text{eV}}\ \text{GeV}^{-1}$$

If QCD axion

$$m_A = 5.70(7)\ \mu\text{eV}\left(\frac{10^{12}\ \text{GeV}}{f_A}\right)$$

Axion-like Particles (ALPs)

- String theory suggests a plentitude of ALPs
- Axion phenomenology can be shared with any other pseudo Nambu-Goldstone bosons (majoron, familon, etc)
- Coupling and axion mass are independent
  - ALPs do not necessarily couple to $G_{\mu\nu}\tilde{G}^{\mu\nu}$
    (nothing to do with PQ mechanism)
  - ALPs will not get masses from QCD effects
- Dark matter candidates
  - WISPs (Weakly Interacting Slim (Sub-eV) Particles)
    - axions
    - ALPs
    - hidden photons (see, also Lab Seminar 20151112)
  - WIMPs (Weakly Interacting Massive Particles)
    - neutralino (SUSY)
      mass ~1-100 GeV

南アルプス市
MINAMI-ALPS CITY

Wide Range of Axion Masses

- Low mass axion is well motivated by cosmology

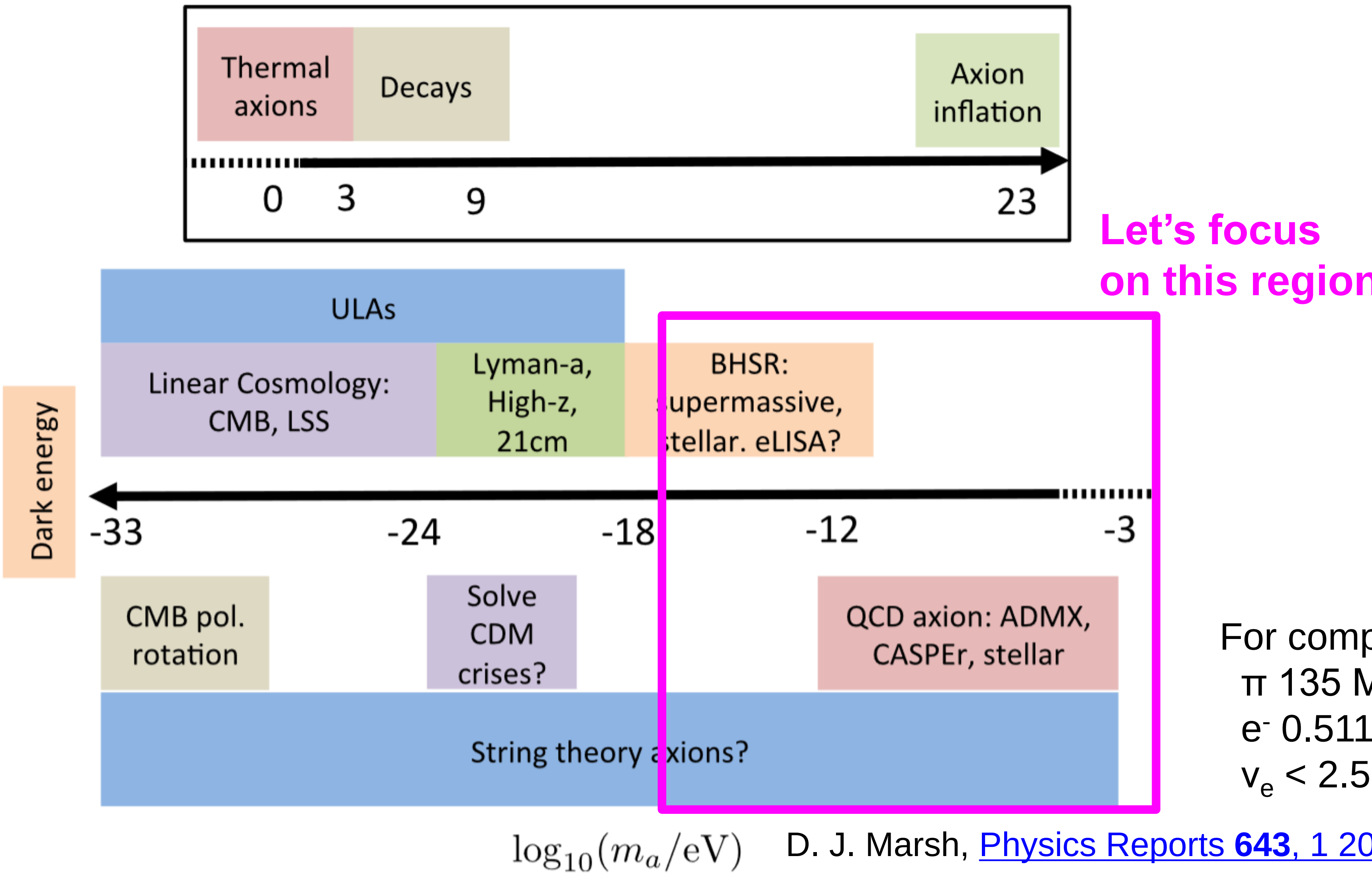

For comparison
π 135 MeV
e^- 0.511 MeV
ν_e < 2.5 eV

D. J. Marsh, Physics Reports **643**, 1 2016

Axion Detection Methods

I. G. Irastorza & J. Redondo [PPNP **102**, 89 (2018)]

Let’s focus on axion-photon coupling

axion-electron

axion-proton/neutron

Detection method	$g_{a\gamma}$	g_{ae}	g_{aN}	$g_{A\gamma n}$	$g_{a\gamma}g_{ae}$	$g_{a\gamma}g_{aN}$	$g_{ae}g_{aN}$	$g_N\bar{g}_N$	Model dependency
Light shining through wall	×								no
Polarization experiments	×								no
Spin-dependent 5th force			×				×	×	no
Helioscopes	×				×	×			Sun
Primakoff-Bragg in crystals	×				×				Sun
Underground ion. detectors	×	×	×			×	×		Sun*
Haloscopes	×								DM
Pick up coil & LC circuit	×								DM
Dish antenna & dielectric	×								DM
DM-induced EDM (NMR)			×	×					DM
Spin precession in cavity		×							DM
Atomic transitions		×	×						DM

Table 3: List of the axion detection methods discussed in the review, with indication of the axion couplings (or product of couplings) that they are sensitive to, as well as whether they rely on astrophysical (axions/ALPs are produced by the Sun) or cosmological (the dark matter is made of axions/ALPs) assumptions. *Also “DM” when searching for ALP DM signals, see section 6.2

Bounds on Axion-Photon Coupling

- black/grey: laboratory (model independent), bluish: depends on stellar physics, greenish: cosmology-dependent

I. G. Irastorza & J. Redondo [PPNP **102**, 89 (2018)]

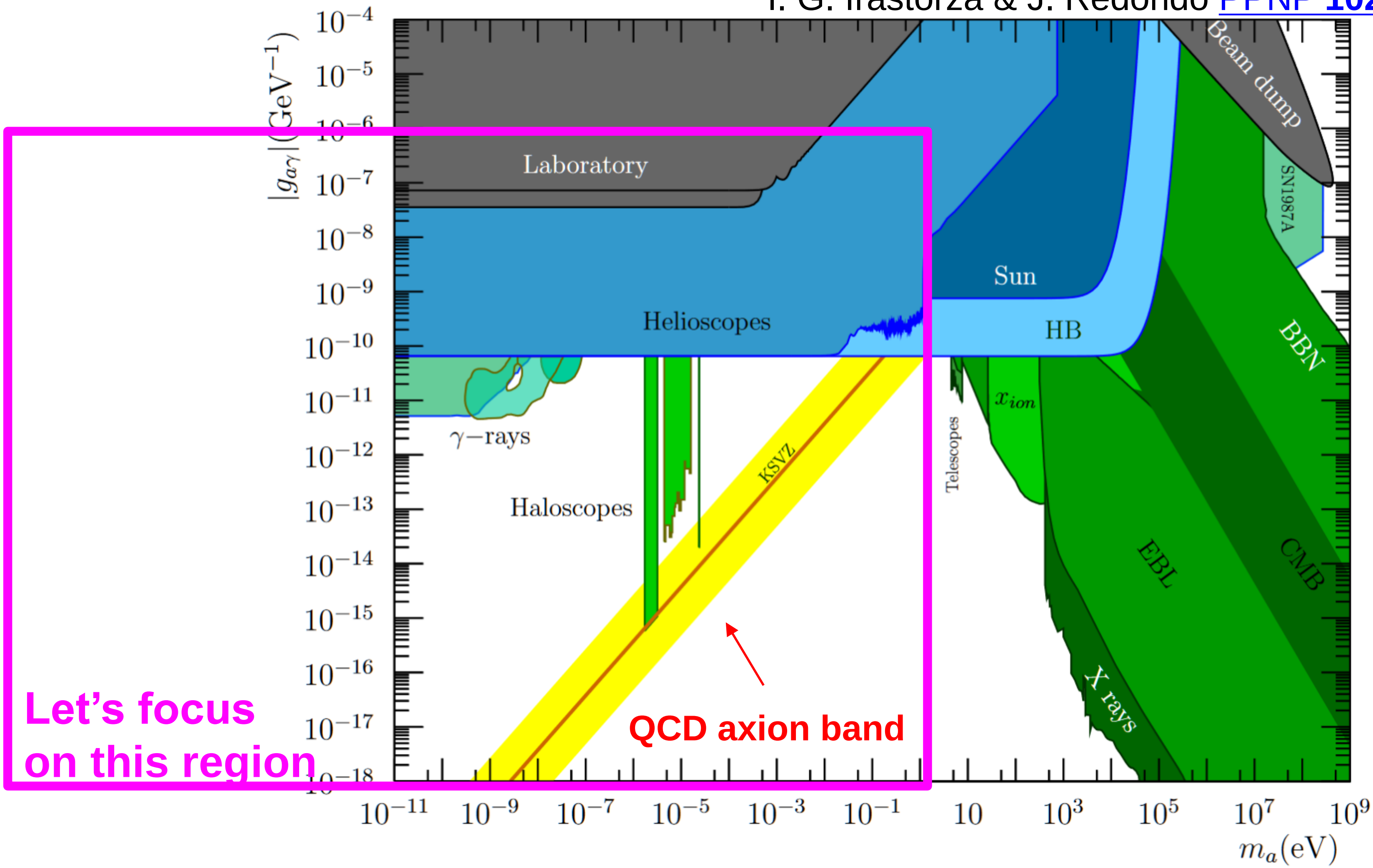

Bounds on Axion-Photon Coupling

- Extracted experiments to be reviewed here

Solid: achieved
Dashed: proposals

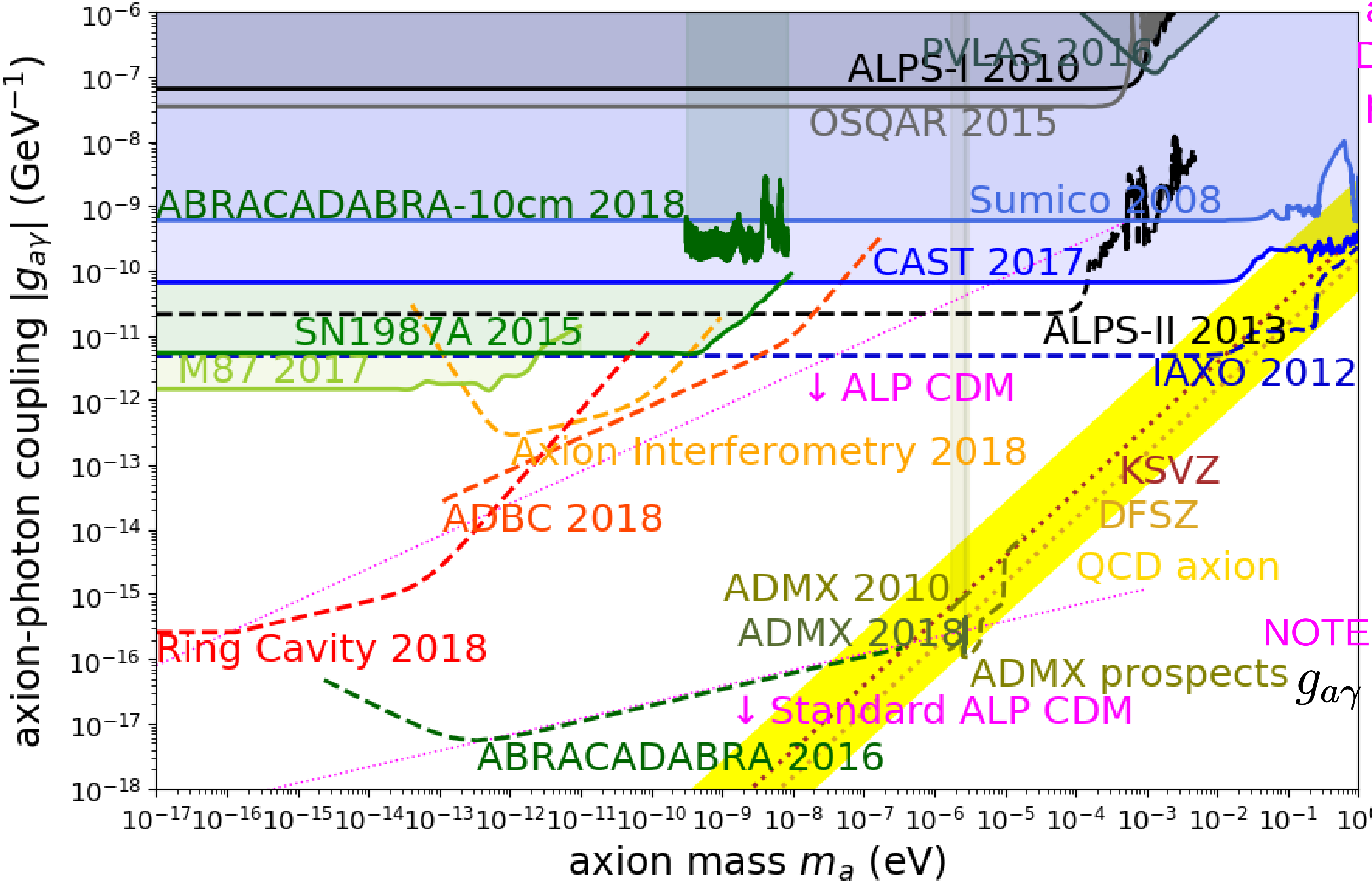

NOTE that $g_{a\gamma} \propto 1/f_a$

Bounds on Axion-Photon Coupling

Light shining through wall experiments

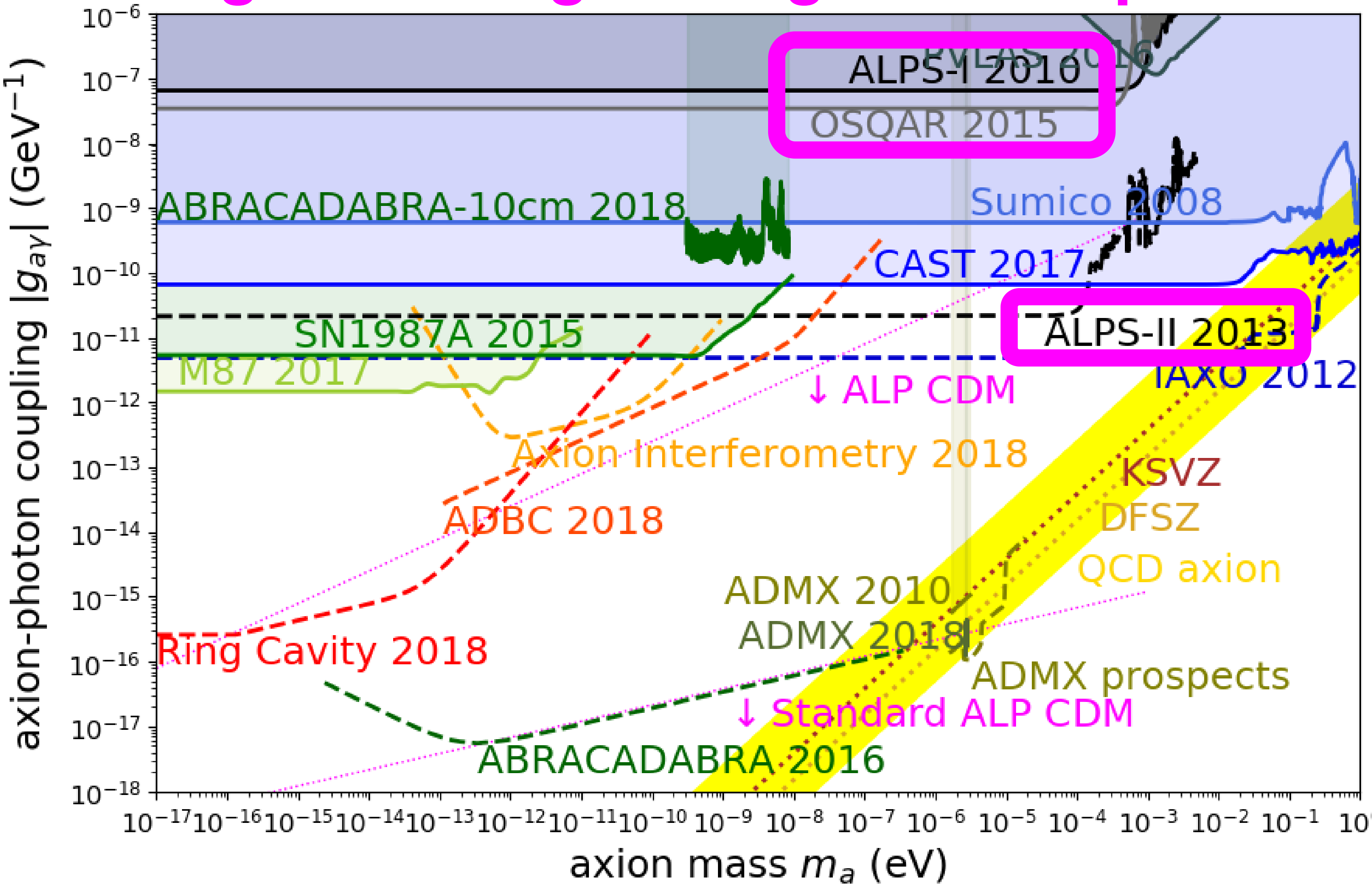

Light Shining through Wall (LSW)

- Axion-photon conversion under magnetic field (Primakoff effect)

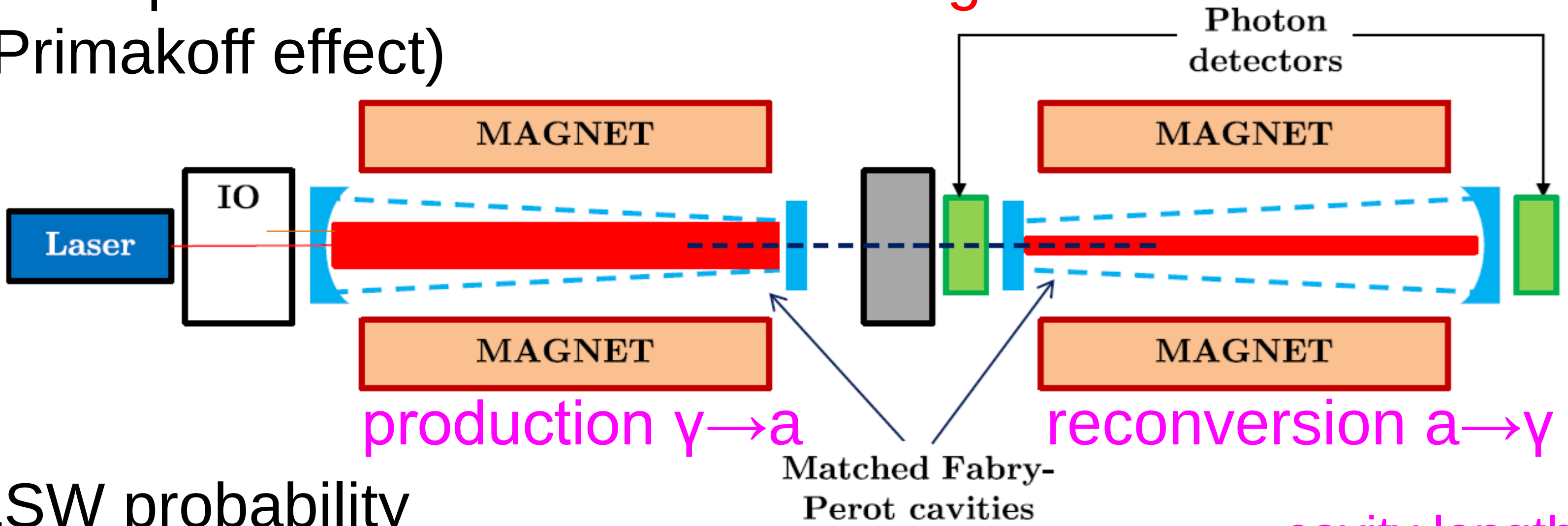

- LSW probability

$$\mathcal{P}(\gamma \to a \to \gamma) = P_p P_r$$

magnetic field

cavity length

momentum transfer

$q = k_\gamma - k_a$

$\sim m_a^2/2\omega$

relativistic limit in vacuum

$$P_{p/r} = \beta_{p/r} \left(\frac{g_{a\gamma} B_e L_{p/r}}{2}\right)^2 \left(\frac{2}{q L_{p/r}}\right)^2 \sin^2\left(\frac{q L_{p/r}}{2}\right)^2$$

power build up

laser frequency

- Maximized when Lp = Lr due to oscillation

Comparison of LSW Experiments

- ALPS at DESY uses HERA magnets
- OSQAR at CERN uses LHC magnets without a cavity
- CROWS and STAX are microwave experiments and can achieve high Q and high power, but L is small

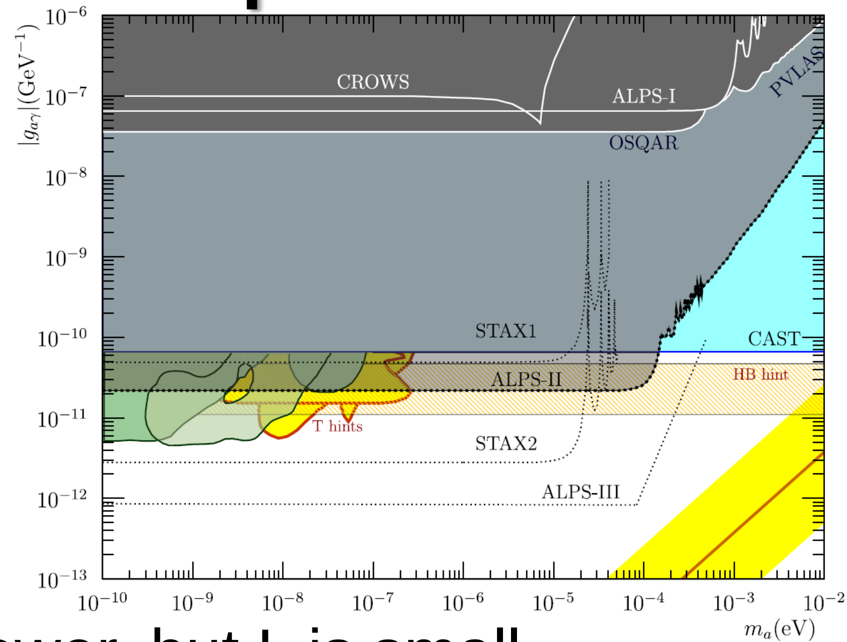

Table 4
List of the most competitive recent LSW results, as well as the prospects for ALPS-II, together with future possible projects, with some key experimental parameters. The last column represents the sensitivity achieved (or expected) in terms of an upper limit on $g_{a\gamma}$ for low m_a. For microwave LSW (CROWS and STAX) the quality factors Q are listed.

Experiment	Status	B (T)	L (m)	Input power (W)	β_P	β_R	$g_{a\gamma}$ [GeV^{-1}]
ALPS-I [433]	Completed	5	4.3	4	300	1	5×10^{-8}
CROWS [435]	Completed	3	0.15	50	10^4	10^4	9.9×10^{-8} ([a])
OSQAR [434]	Ongoing	9	14.3	18.5	–	-	3.5×10^{-8}
ALPS-II [436]	In preparation	5	100	30	5000	40000	2×10^{-11}
ALPS-III [437]	Concept	13	426	200	12500	10^5	10^{-12}
STAX1 [438]	Concept	15	0.5	10^5	10^4	–	5×10^{-11}
STAX2 [438]	Concept	15	0.5	10^6	10^4	10^4	3×10^{-12}

[a] The limit is better for specific m_a values, see Fig. 6.

ALPS I (2010)

[Phys. Lett. B **689**, 31 (2010)]

- Any Light Particle Search

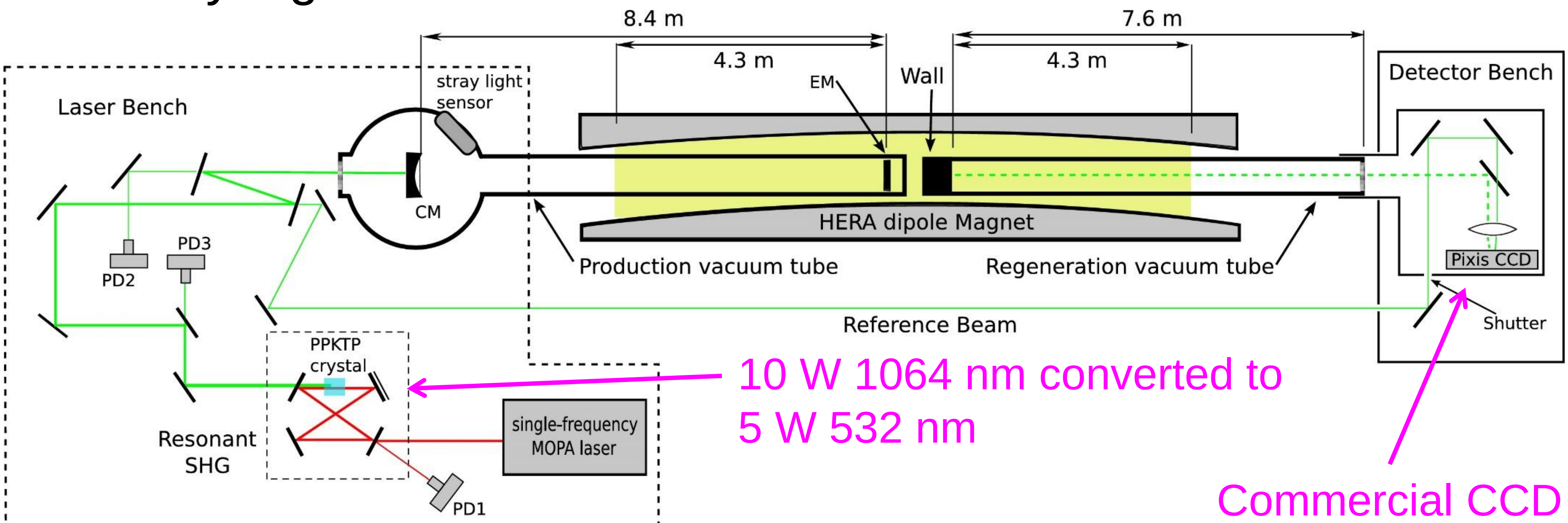

10 W 1064 nm converted to 5 W 532 nm

Commercial CCD camera with 96% QE at -70℃

Why CCD?

CCD used probably to fit data with Gaussian to reduce uncertainty

[https://alps.desy.de/e141063/]

ALPS I (2010)

Phys. Lett. B **689**, 31 (2010)

- Also sensitive to hidden photon with magnets off
- Different argon pressure to change refractive index which affects WISP-photon oscillations

Magnet	Laser Pol.	# frames	Pressure/mbar	$n-1$	Power/W	Prob. 95% limit	0^-	0^+	γ'	MCP
On	Par.	5/6	$< 10^{-5}$	0	1096	2.25×10^{-25}	✓	–	–	✓
On	Par.	8	0.18	5.0×10^{-8}	1044	10.8×10^{-25}	✓	–	–	✓
On	Perp.	9/5/2	$< 10^{-5}$	0	1088	2.08×10^{-25}	-	✓	-	✓
On	Perp.	8	0.18	5.0×10^{-8}	954	5.22×10^{-25}	–	✓	–	✓
Off (1 + 3)	Par. + Perp.	27	$< 10^{-5}$	0	1121	1.14×10^{-25}	–	–	✓	-
Off	Par.	9	0.11/0.14	$3.1/3.9 \times 10^{-8}$	968	3.11×10^{-25}	–	–	✓	-

ALPs

hidden photon

mini-charged particles

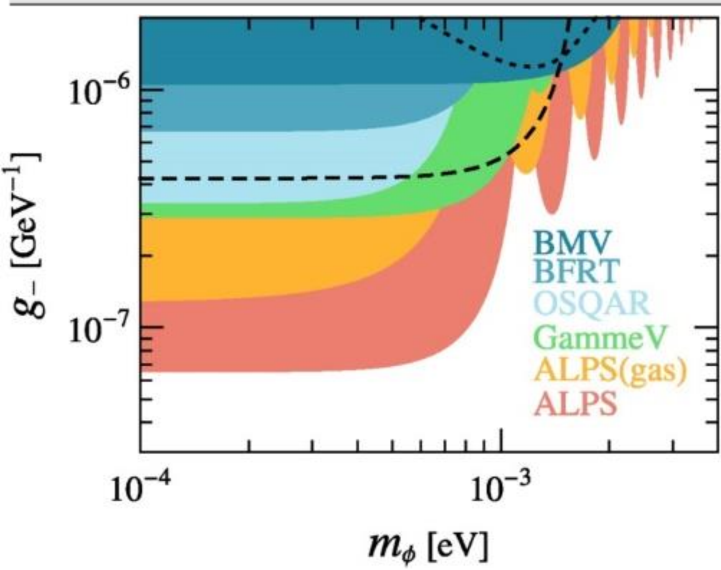

bound on pseudoscalar ALPs (axion is pseudoscalar)

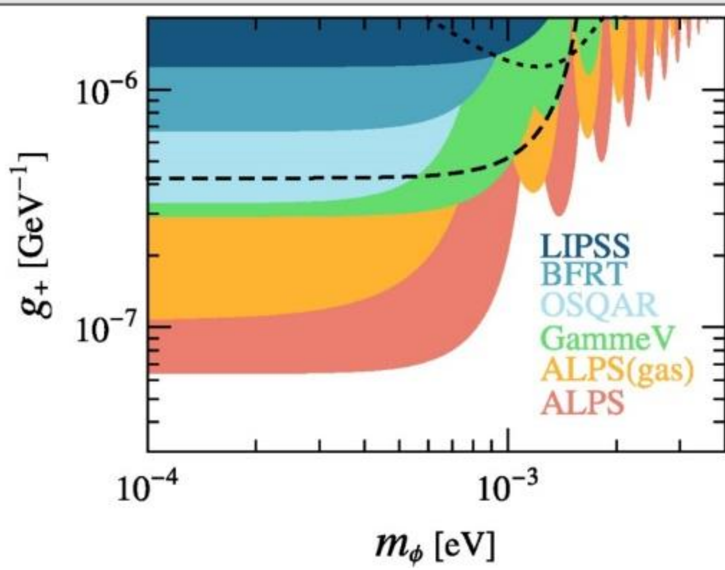

bound on scalar ALPs

OSQAR (2015)

PRD **92**, 092002 (2015)

- Optical Search for QED Vacuum Birefringence, Axions and Photon Regeneration

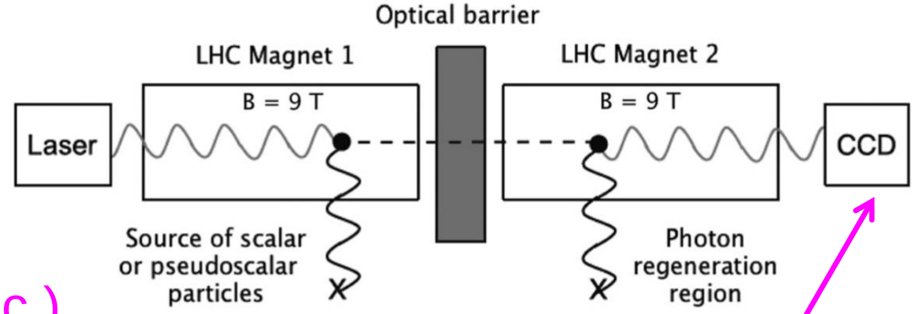

FIG. 1. Principle of the OSQAR LSW experiment.

18.5 W 532 nm
(Verdi V18 from Coherent Inc.)

QE 88% at -92°C
(overall efficiency 56%)

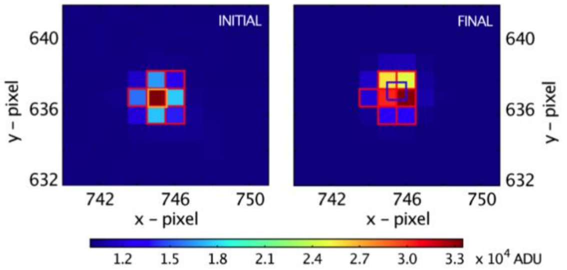

FIG. 2 (color online). Initial and final positions of the attenuated laser beam on the CCD for run-90 devoted to the search of S-ALPs ($\vec{E}_\gamma \perp \vec{B}$). The signal region covers seven pixels.

Beam position before and after each run was measured and fitted with Gaussian to see beam position drift

https://ep-news.web.cern.ch/content/osqar-experiment-sheds-light-hidden-sector-cern%E2%80%99s-scientific-heritage

Bounds on Axion-Photon Coupling

Polarization measurements

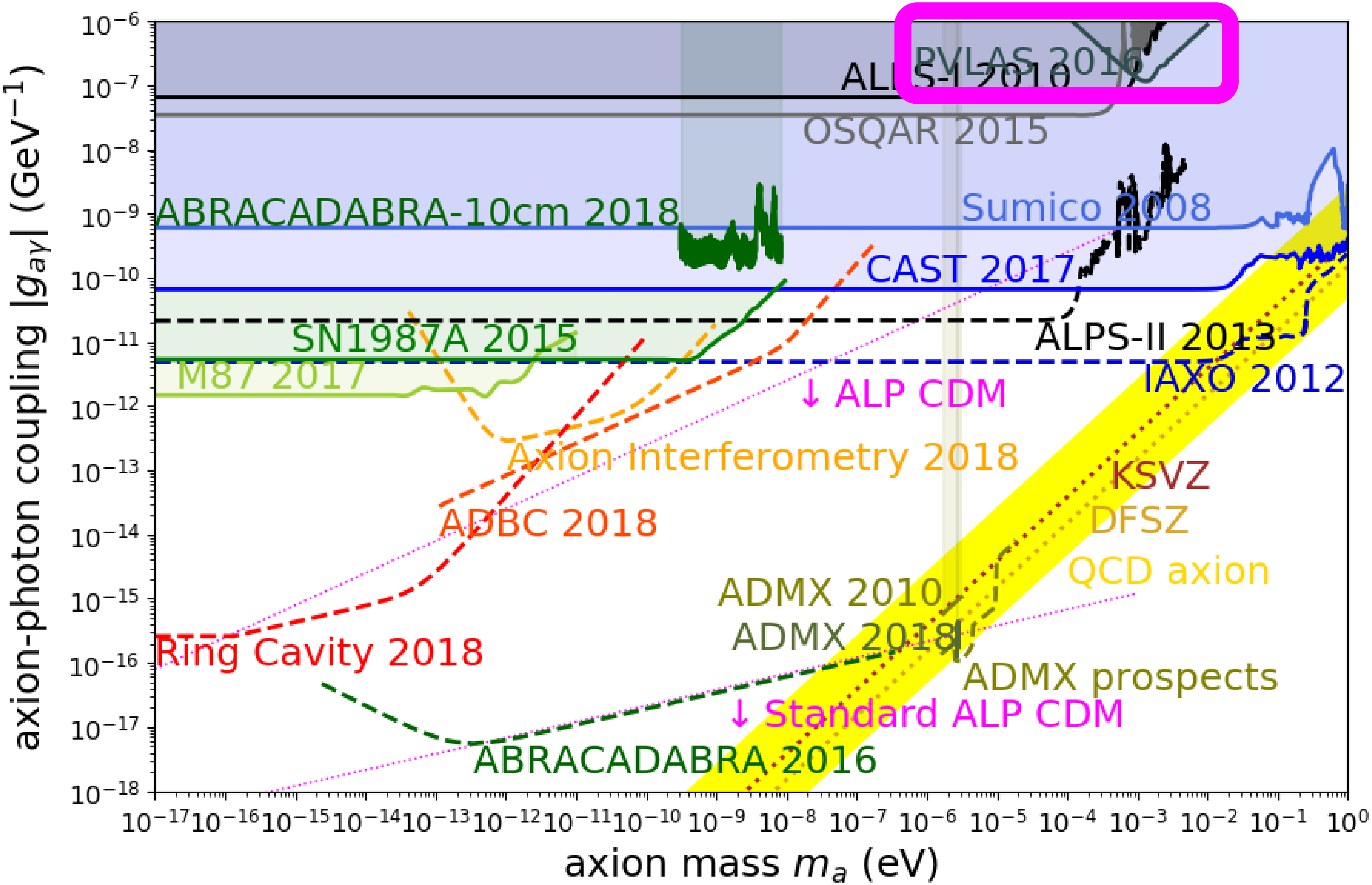

Polarization Measurements

- Search for vacuum birefringence
- QED birefringence will be a background (although not yet reached)

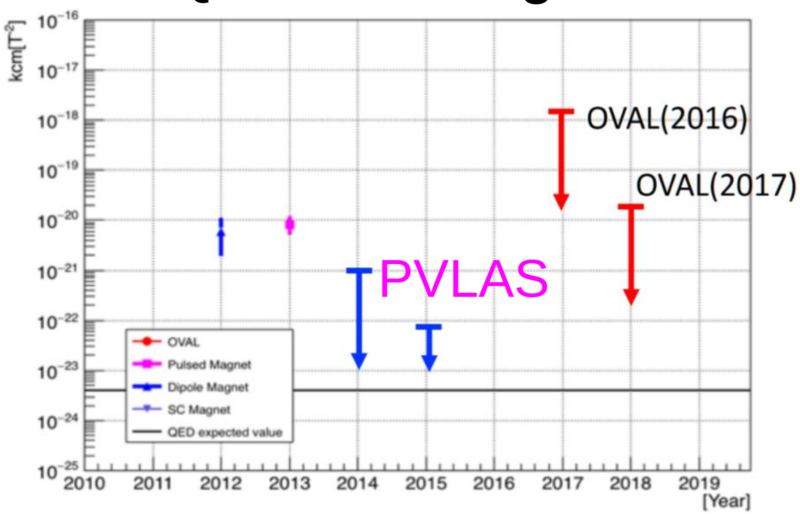

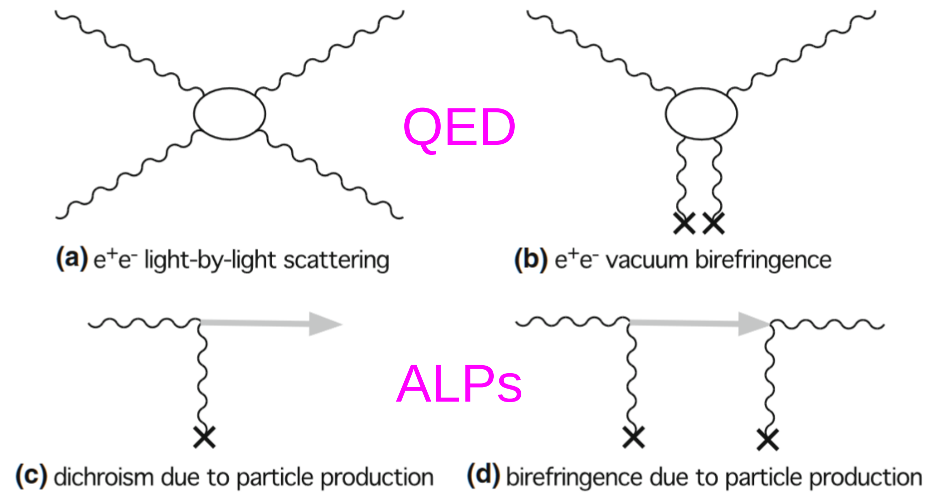

Fig. 1 Lowest order elementary processes leading to magnetic birefringence and dichroism

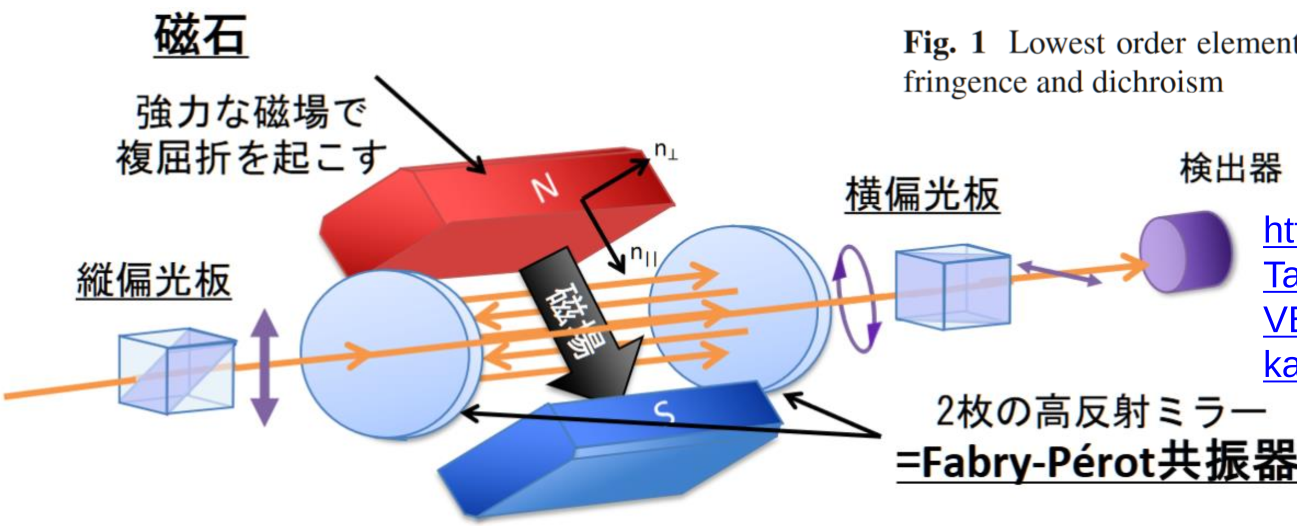

https://tabletop.icepp.s.u-tokyo.ac.jp/Tabletop_experiments/VB__Pulsed_magnets+laser_files/kamioka-jps2018autumn.pdf

PVLAS (2016)

Eur. Phys. J. C **76**, 24 (2016)

- Polarizzazione del Vuoto con LASer
- Currently limited by thermal effects in mirror's birefringence

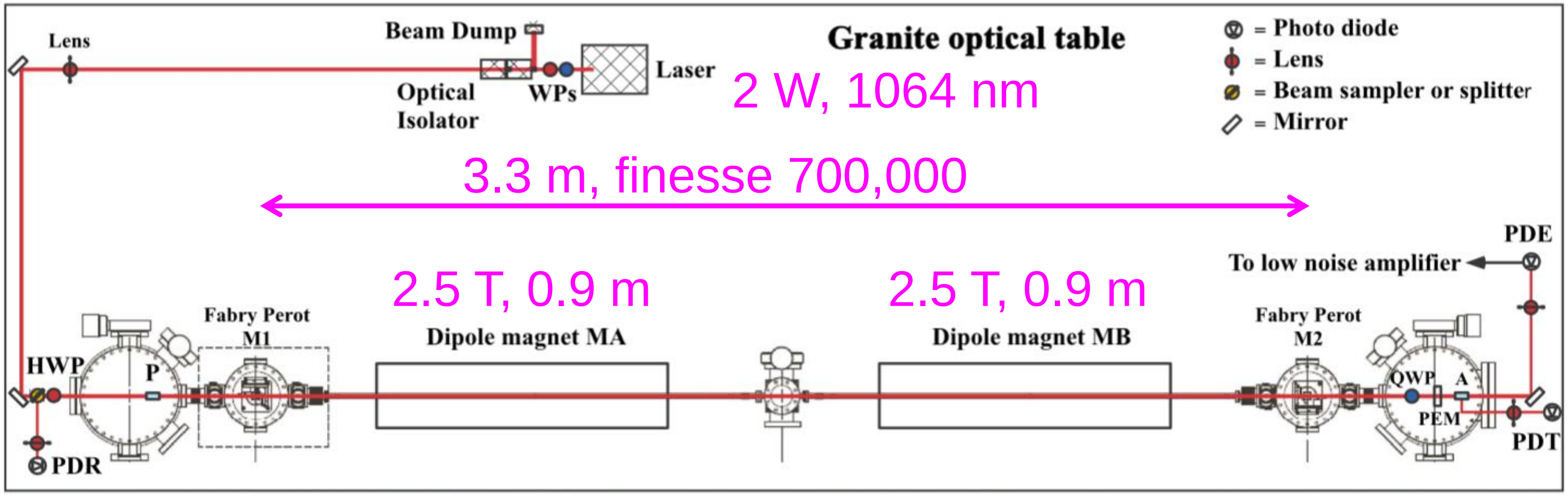

Always some light on PD due to birefringence of cavity mirror and this background fluctuates from thermal effects

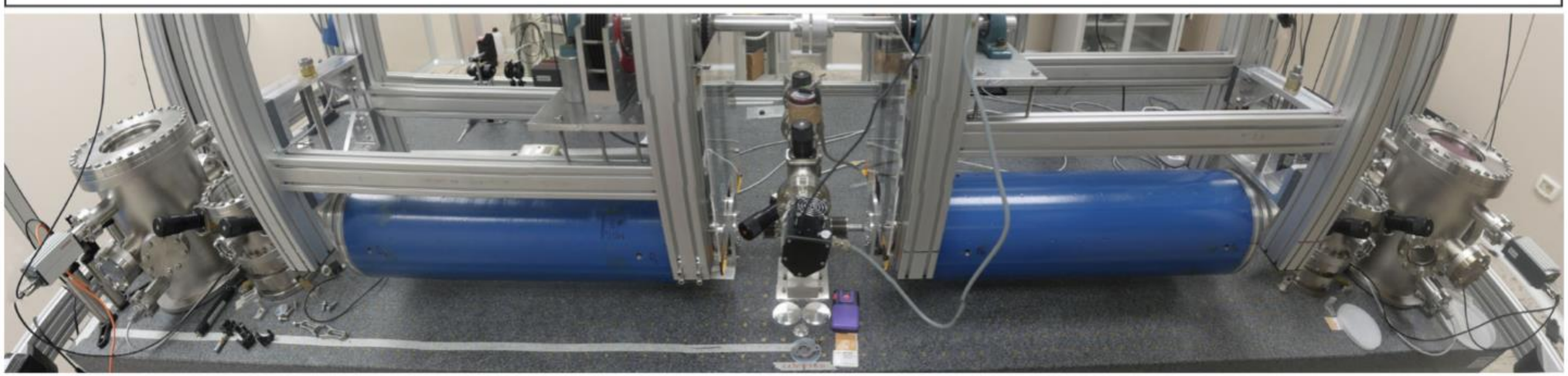

For comparison, OVAL (2017) 9 T, 0.2 m Finesse 350,000

Fig. 6 *Upper panel* Optical and mechanical scheme of the apparatus. *WPs* wave-plates, *HWP* half-wave-plate, *PDR* reflection photodiode, *P* polariser, *Ms* mirrors, *QWP* quarter-wave-plate, *PEM* photoelastic modulator, *A* analyser, *PDT* transmission photodiode, *PDE* extinction photodiode. *Lower panel* A wide-angle picture of the PVLAS apparatus. *The two blue cylinders* are the permanent magnets

Bounds on Axion-Photon Coupling

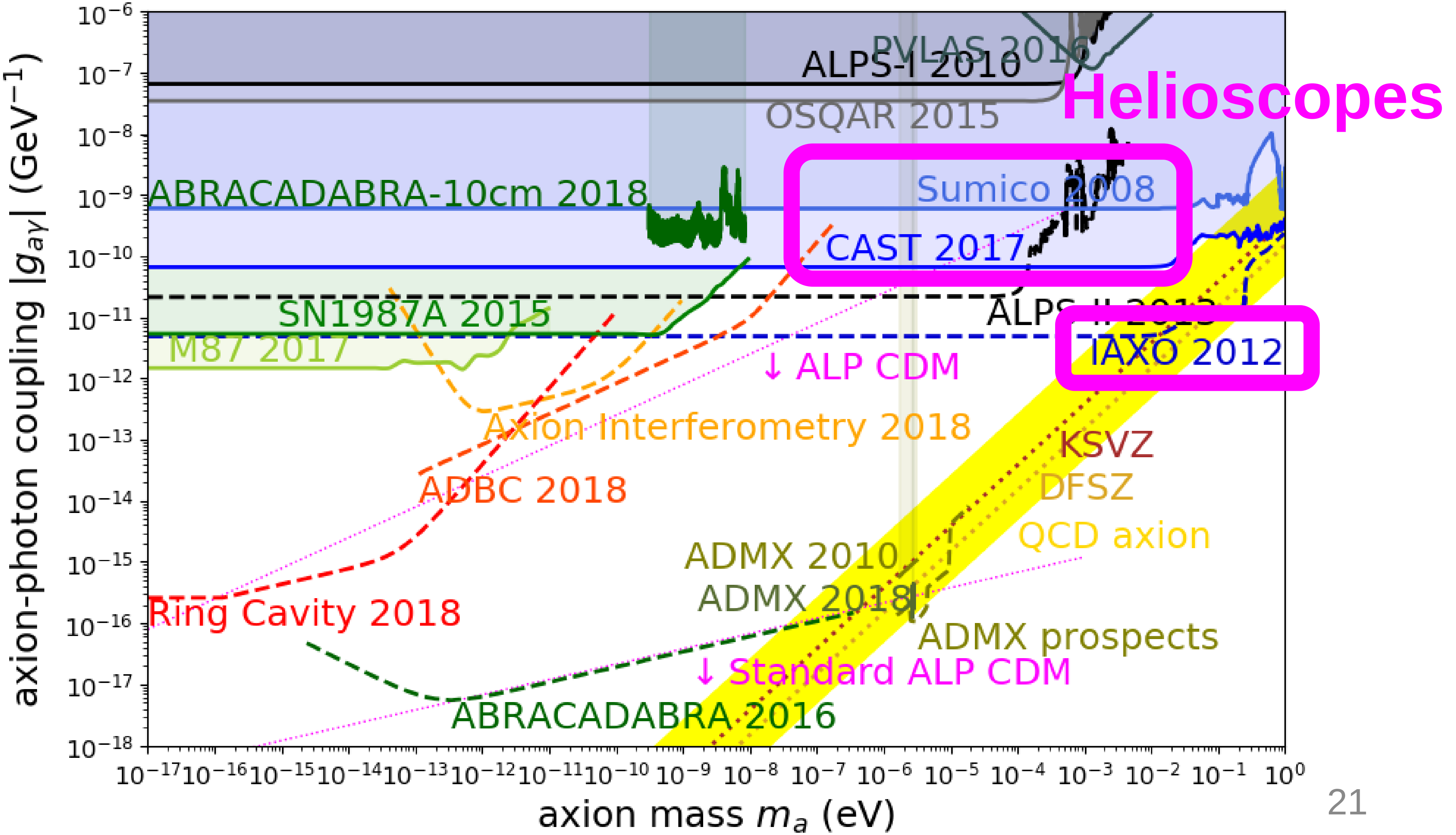

Helioscopes

- Detect solar axions
  - produced from Primakoff conversion of plasma photons into axions in the Coulomb field of charged particles
  - and from ALPs to electron coupling

Assumption of ALP-electron effect being small OK?

- Convert solar axions into X-rays with magnets
- Helioscope searches are dependent on solar axion generation process (Primakoff contribution is robust prediction depending only on well known solar physics)

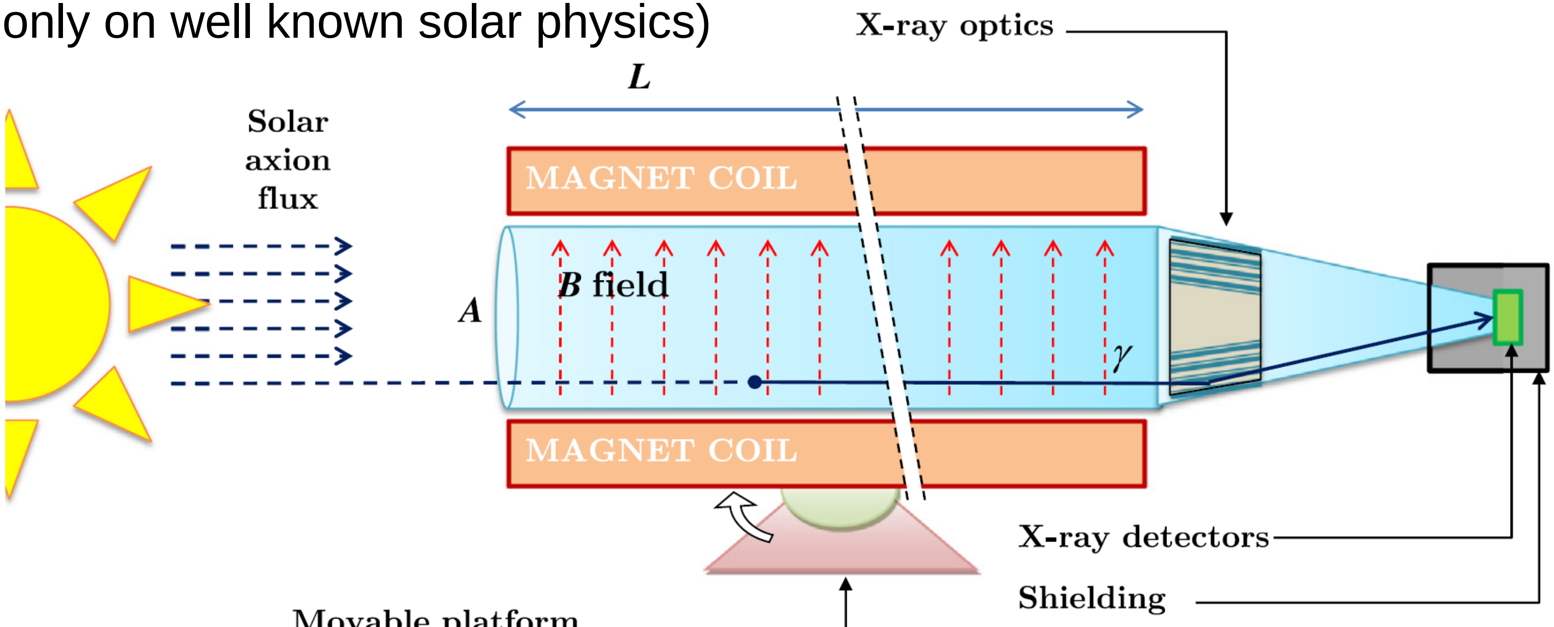

Comparison of Helioscopes

- 1G: Brookhaven
- 2G: Sumico at UTokyo
- 3G: CAST at CERN
- 4G (future): IAXO at CERN

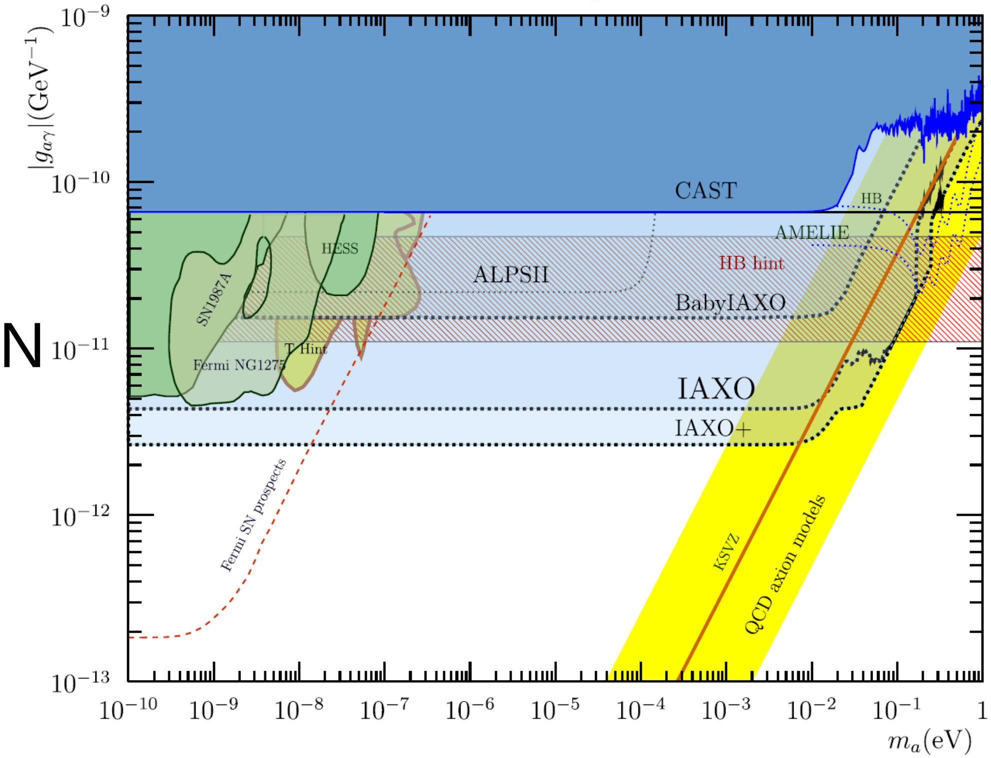

Table 5

List of past and future helioscopes with some key features. The last column represents the sensitivity achieved (or expected) in terms of an upper limit on $g_{10} = g_{a\gamma} \times 10^{10}$ GeV for low m_a. The numbers for the TASTE, BabyIAXO and IAXO helioscopes correspond to the design parameters considered in the quoted references.

Experiment	References	Status	B (T)	L (m)	$\mathcal{A}$ (cm^2)	Focusing	g_{10}
Brookhaven	[38]	Past	2.2	1.8	130	No	36
SUMICO	[46,486]	Past	4	2.5	18	No	6
CAST	[481,483,488,491,492]	Ongoing	9	9.3	30	Partially	0.66
TASTE	[499]	Concept	3.5	12	2.8×10^3	Yes	0.2
BabyIAXO	[500]	In design	∼2.5	10	2.8×10^3	Yes	0.15
IAXO	[487,501]	In design	∼2.5	22	2.3×10^4	Yes	0.04

Sumico (1998,2002,2008)

Phys. Lett. B 434, 147 (1998)
Phys. Lett. B 536, 18 (2002)
Phys. Lett. B 668, 93 (2008)

- Dynamic tracking of the Sun
(50% of the time)
- In vacuum, sensitivity is worse for higher axion mass

$$\mathcal{P}(a\to\gamma) = \left(\frac{g_{a\gamma}B_e L}{2}\right)^2 \left(\frac{2}{qL}\right)^2 \sin^2\left(\frac{qL}{2}\right)$$

$$q = k_\gamma - k_a \sim (m_\gamma^2 - m_a^2)/2\omega = m_a^2/2\omega$$

in vacuum

- Effective m_γ can be increased with buffer gas

$$m_\gamma = 4\pi\alpha N_e m_e$$

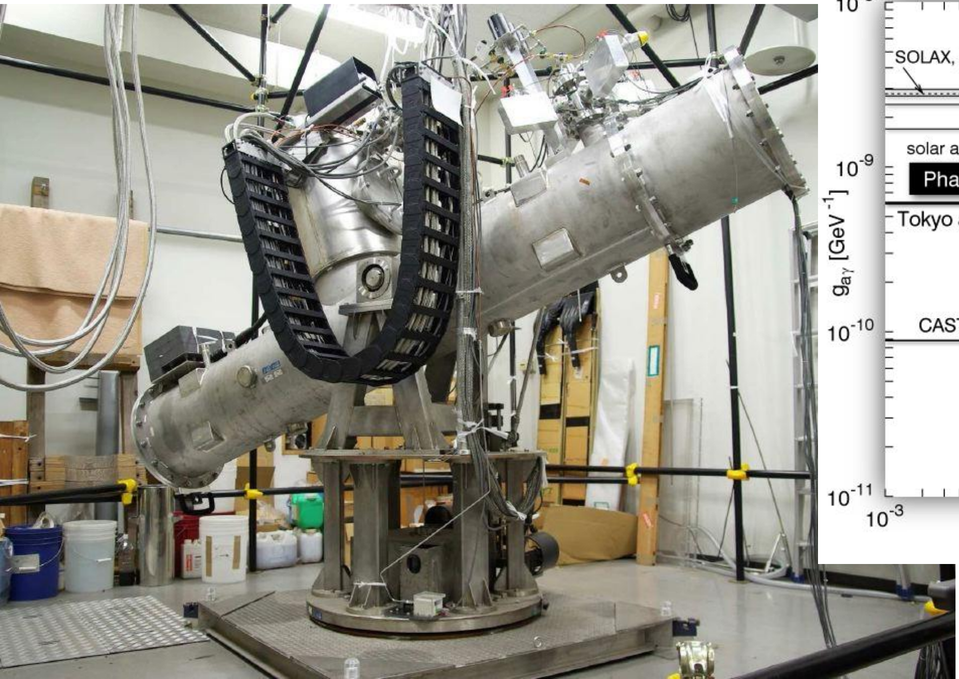

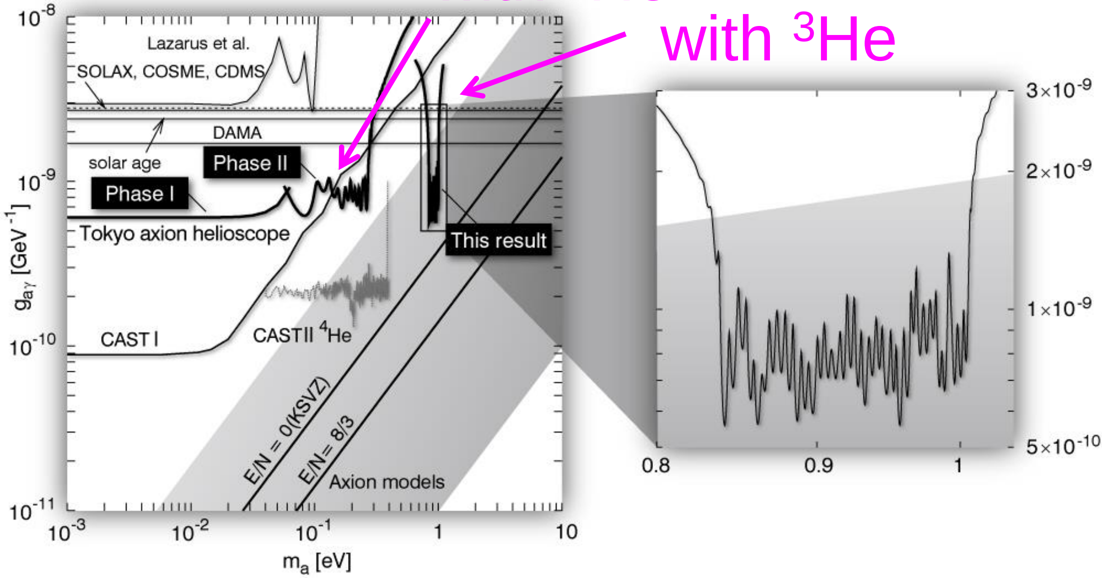

http://www.icepp.s.u-tokyo.ac.jp/~minowa/Minowa_Group.files/sumico.htm

CAST (2003-)

- CERN Axion Solar Telescope
- In vacuum (2003-2004)
- With ^{4}He (2005-2006)
- With ^{3}He (2008-2011)
- Improved detectors and X-ray optics (2013-2015)

[Nature Physics **13**, 584 (2017)]

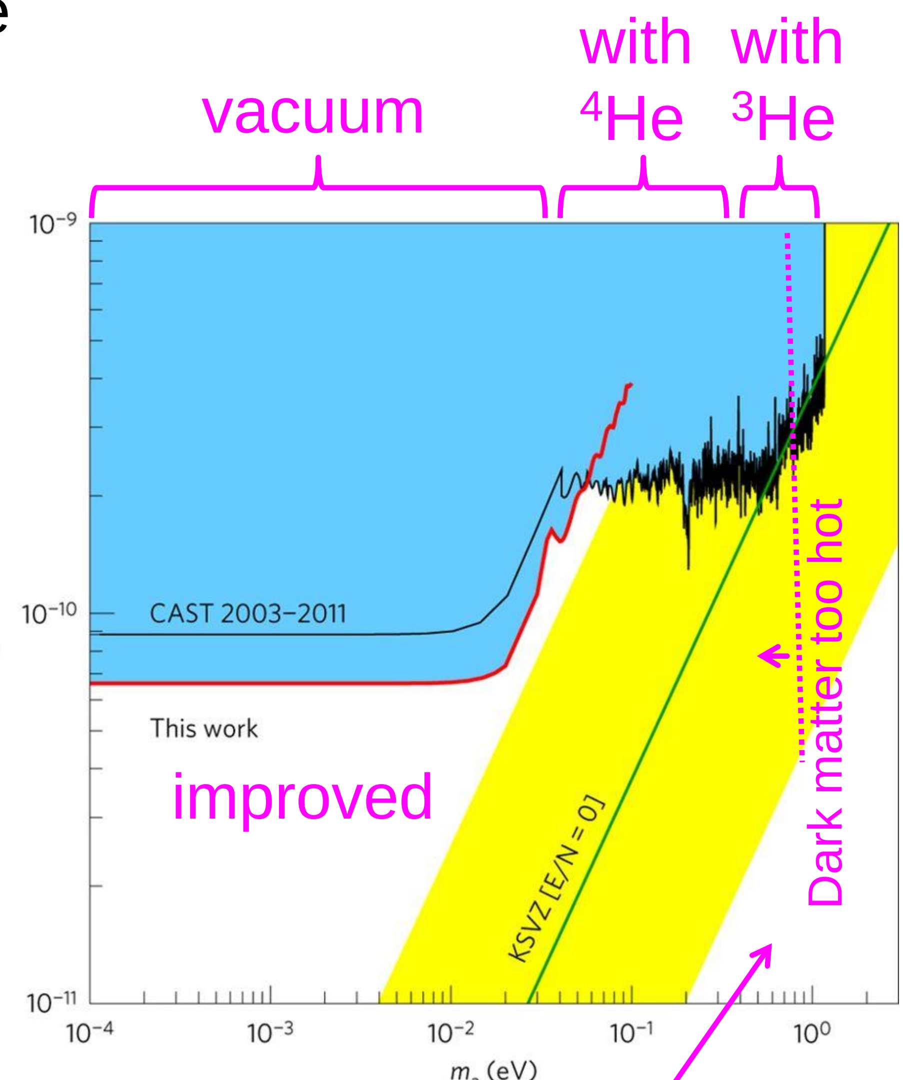

??

from WMAP
JCAP 08, 001 (2010)

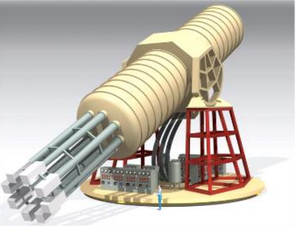

IAXO (Proposed 2011)

JINST 9, T05002 (2014)

- International Axion Observatory
- Powerful magnet from ATLAS
- Improved optics similar to NASA’s NuSTAR

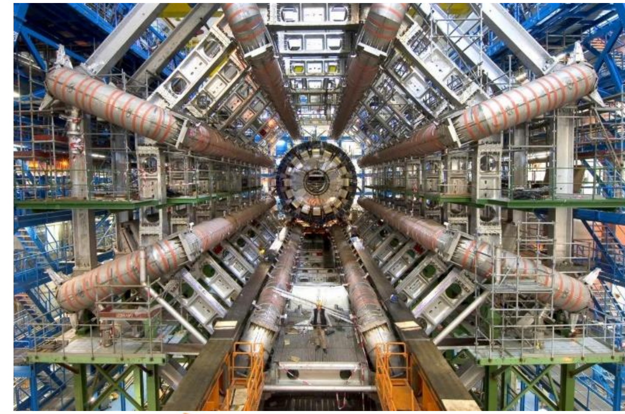

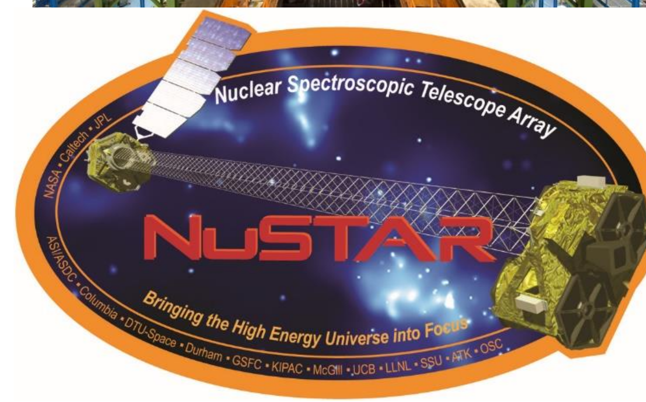

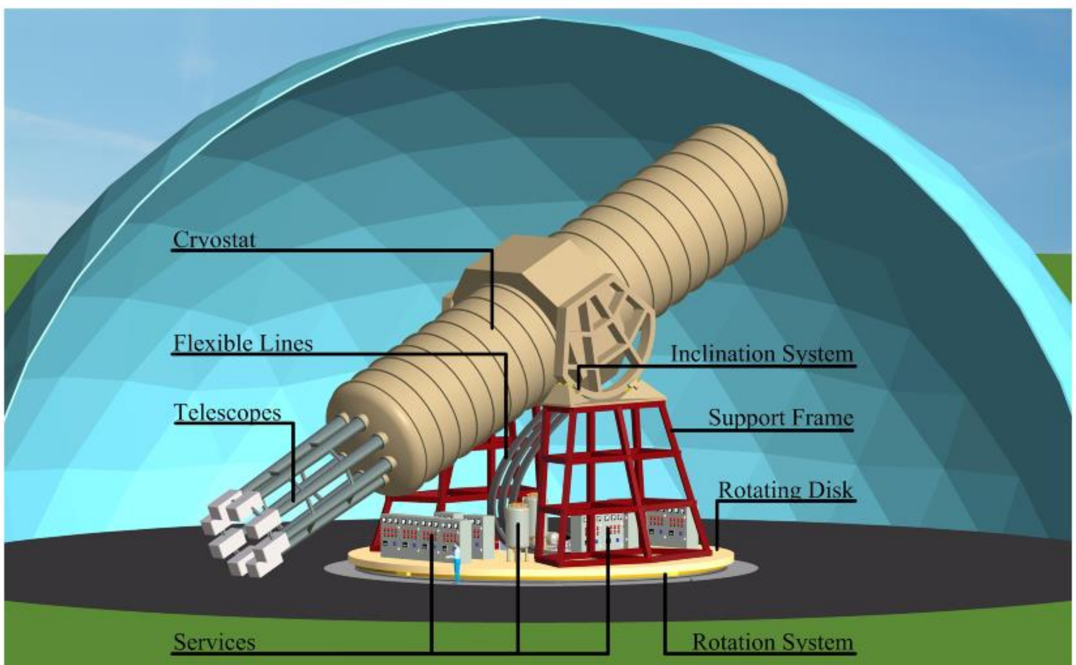

Bounds on Axion-Photon Coupling

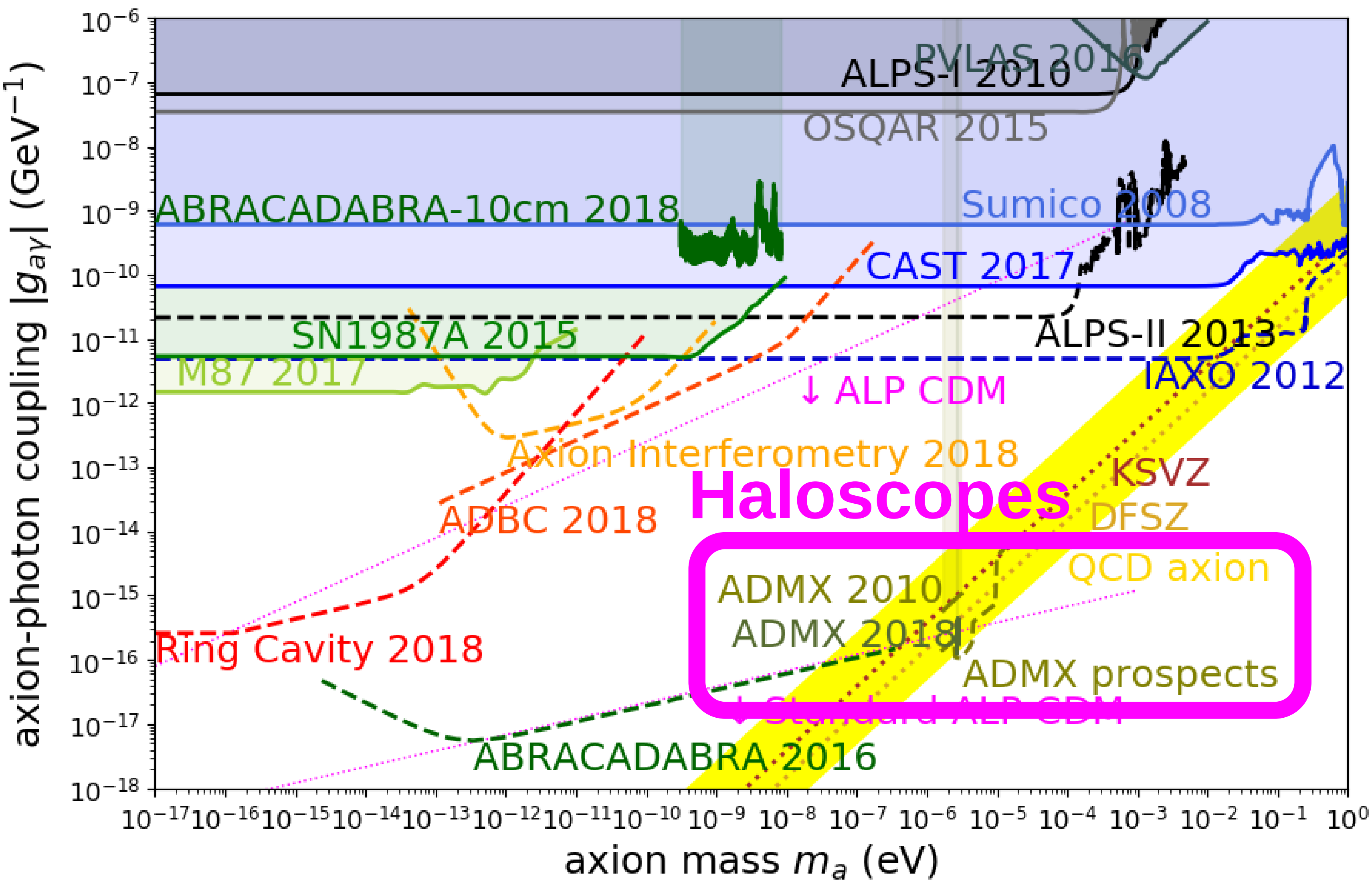

Dark Matter Axion Searches

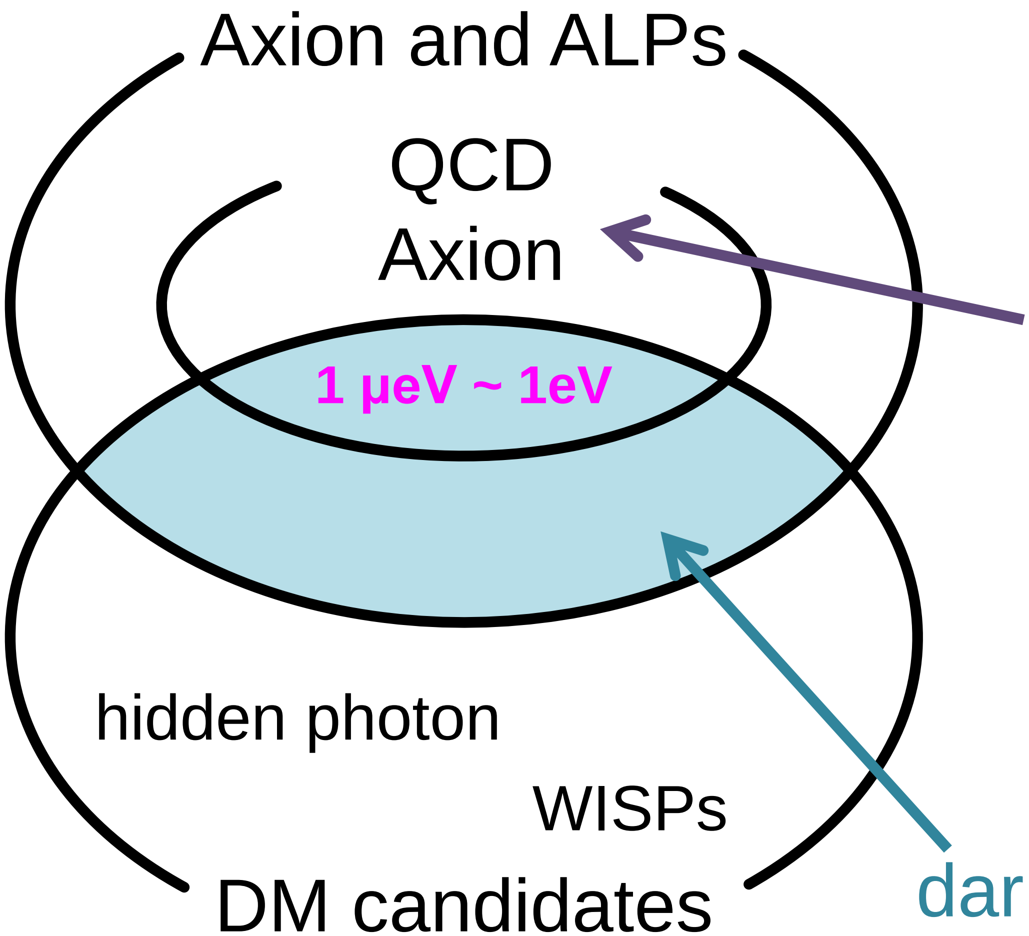

axion which solves strong CP problem

dark matter axion searches look for this region (including ours)

Haloscopes

- Dark matter axion detection with resonant microwave cavities
  - narrow mass range due to resonant detection
- Haloscope searches assume Milkey Way dark matter halo is entirely composed of ALPs
  (upper limit on $g_{a\gamma}\sqrt{\tilde{\varrho}_a}$, but assumes $\tilde{\varrho}_a \equiv \varrho_a/\varrho = 1$)

local ALP density

local DM density (0.45 GeV/cm^3)

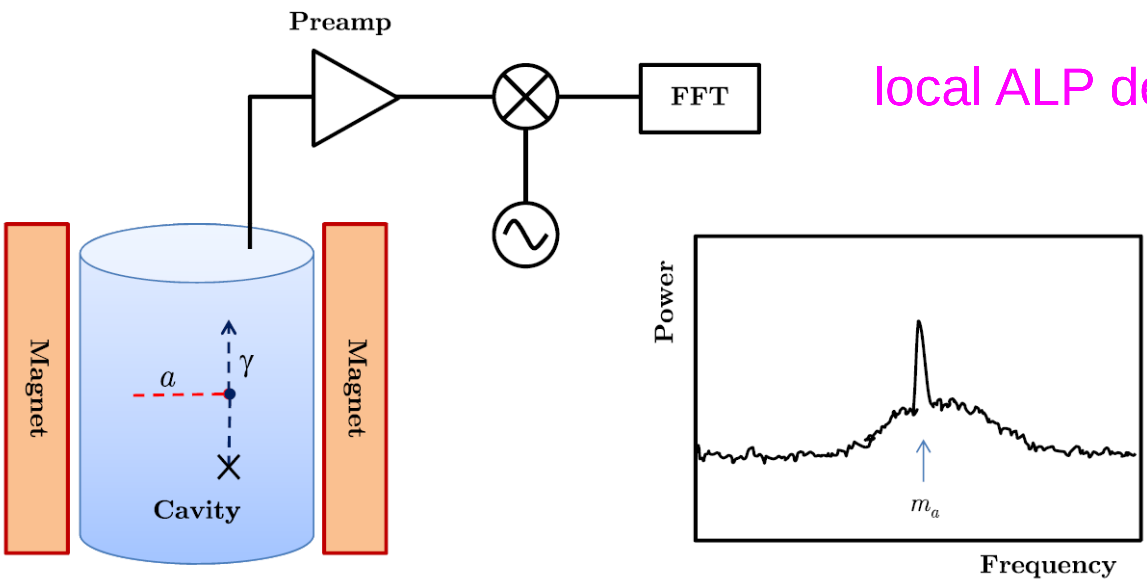

Fig. 14. Conceptual arrangement of an axion haloscope. If m_a is within $1/Q$ of the resonant frequency of the cavity, the axion will show as a narrow peak in the power spectrum extracted from the cavity.

Haloscope Experiments

- Many experiments with different resonant frequency
- ADMX at UWash is leading experiment
- Lower frequency is tough since it requires larger cavity with larger magnet
- Higher frequency is tough since it requires smaller cavity with smaller signal

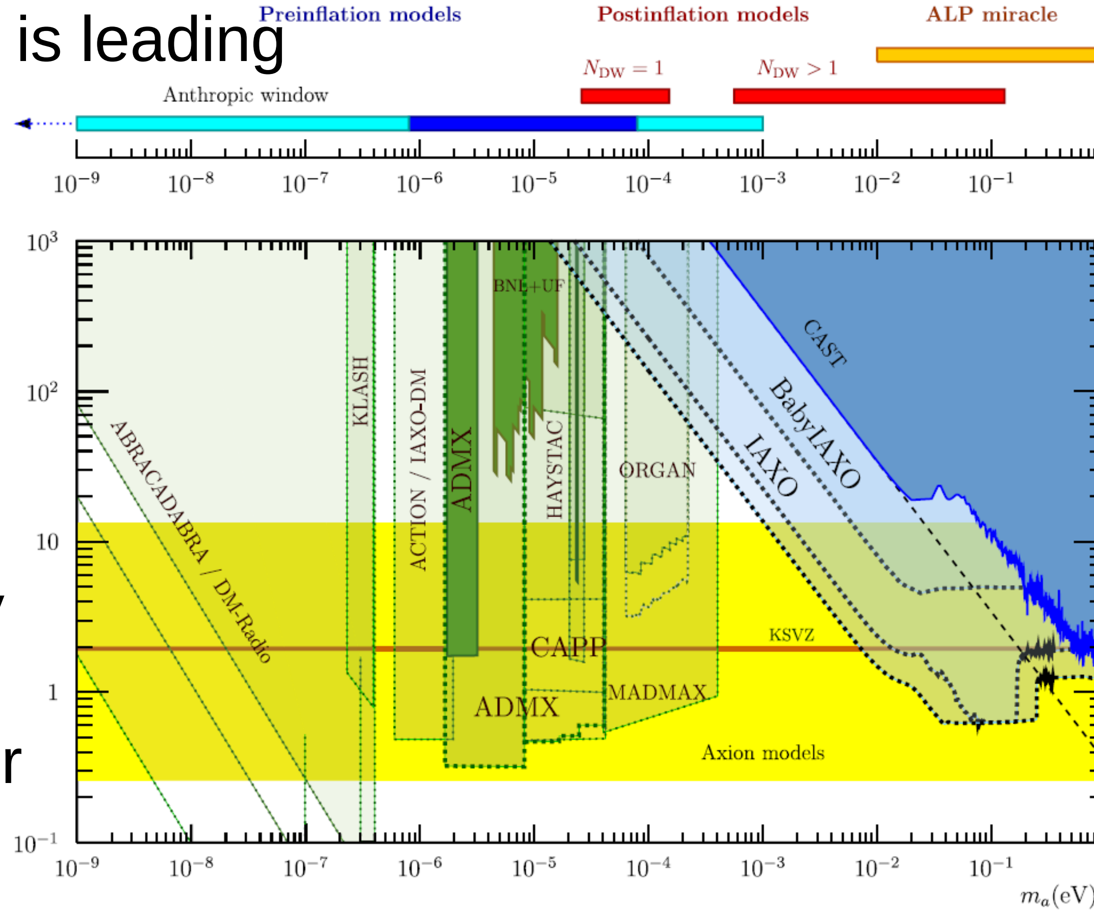

Fig. 18. Exclusion regions from haloscope searches (in green) expressed in terms of $|C_{a\gamma}|\sqrt{\tilde{\varrho}_a}$. We display $C_{a\gamma}$ in the sense of $C_{a\gamma} = g_{a\gamma} f_A(2\pi/\alpha)$ from (2.42) by rescaling sensitivities on $g_{a\gamma}$ by the known relation between f_A, m_A. Some of the regions tentatively within reach of future experiments are indicated as semi-transparent green areas. Some of those regions are dependent, to different extents, on successful completion of R&D on novel detection concepts, as explained in the text. Regions explored and projected by helioscopes are also shown (in blue). As usual the yellow band and orange line represent the QCD axion models and the benchmark KSVZ model respectively. The sketch on top shows the mass ranges for which total DM density can be obtained in different models, as explained in Section 3.1.1. (For interpretation of the references to colour in this figure legend, the reader is referred to the web version of this article.)

ADMX (1995-)

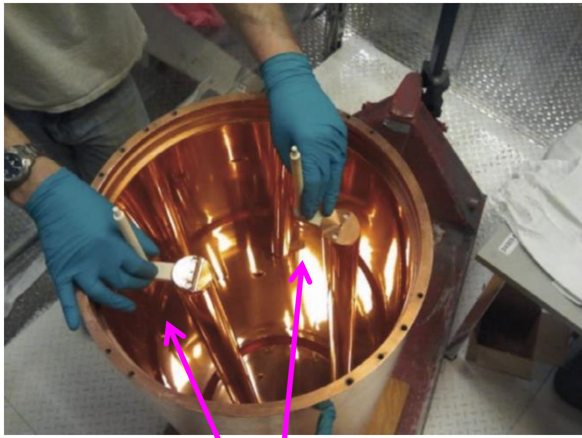

- Axion Dark Matter eXperiment
- Latest result in [PRL **120**, 151301 (2018)]

  1995-2004: cooled to 1.5K, HFET readout
  T_{sys} ~ 3 K
  2007-2009: SQUID employed
  2017: cooled to 150 mK,
  T_{sys} ~ 500 mK

Why SQUID?

Probably used to detect small current

resonant frequency tuning rod

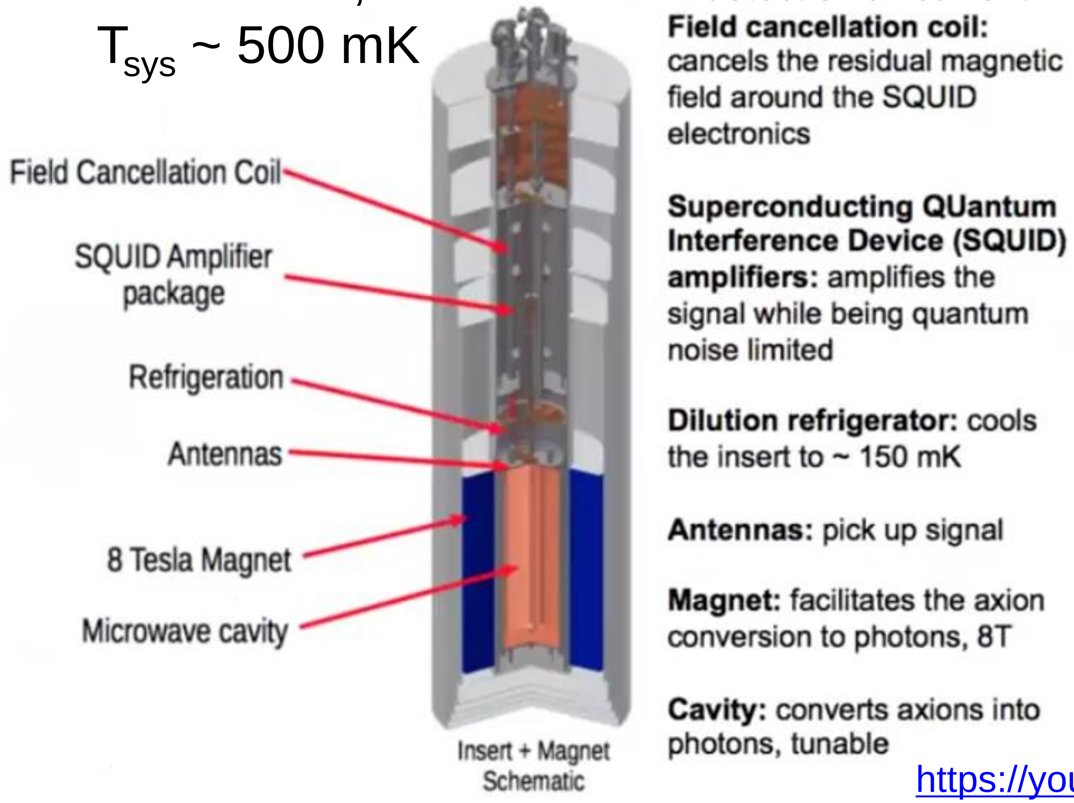

https://youtu.be/_WAnjdlFF1k

Bounds on Axion-Photon Coupling

Low frequency resonators with LC circuits

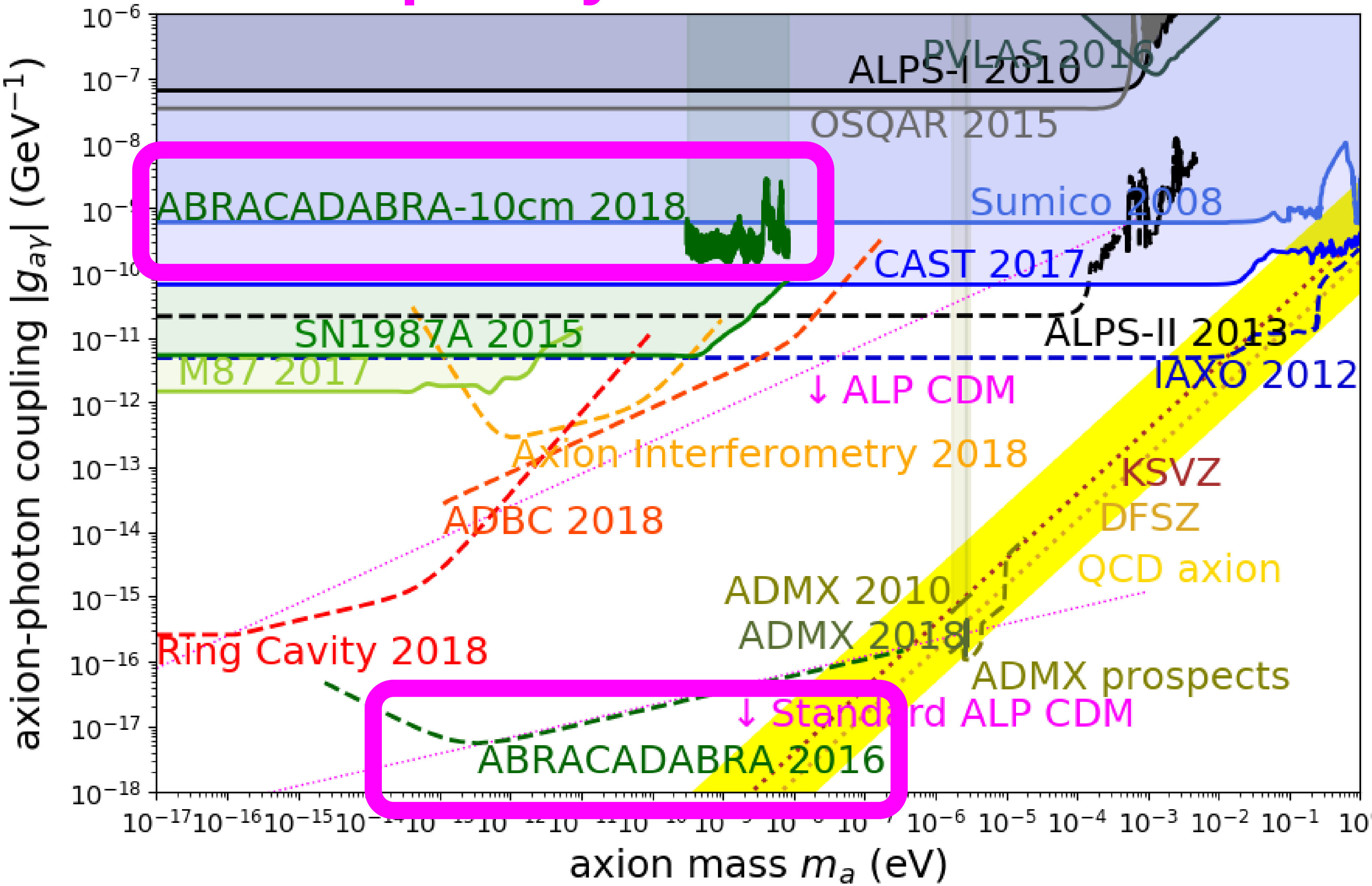

Low Frequency Resonators with LC

- Detect oscillating magnetic field generated by dark matter axions in an external homogeneous magnetic field

$$\mathbf{B}_a = \frac{1}{i\omega}\nabla \times \mathbf{E}_a = -g_{a\gamma}\mathbf{v} \times \mathbf{B}_e a$$

axion field

$$a(t) = a_0 \cos\left(m_a t + \delta_\tau(t)\right)$$

axion DM velocity (10^{-3})

external magnetic field

- Also assumes ALP density = dark matter density

- ABRACADABRA experiment at MIT
  toroidal magnet gives no background magnetic field at the center

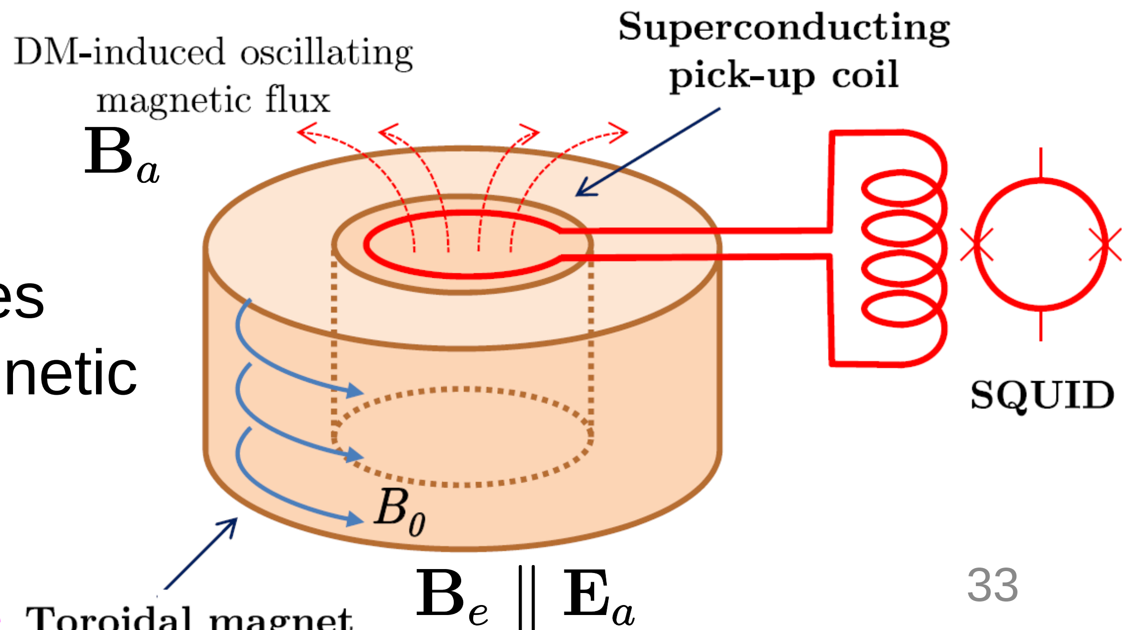

Why not directly by SQUID?

Probably SQUID requires lower temperature

Maxwell-Axion Equations

PRL **51**, 1415 (1983), JCAP **01**, 061 (2017)

- Maxwell equations in the presence of axions

$$\nabla \cdot \mathbf{E} = \rho_Q - \boxed{g_{a\gamma} \mathbf{B} \cdot \nabla a}$$

$$\nabla \times \mathbf{B} - \frac{\partial \mathbf{E}}{\partial t} = \mathbf{J} + \boxed{g_{a\gamma} \left(\mathbf{B} \frac{\partial a}{\partial t} - \mathbf{E} \times \nabla a \right)}$$

$$\nabla \cdot \mathbf{E} = 0$$

$$\nabla \times \mathbf{E} + \frac{\partial \mathbf{B}}{\partial t} = 0$$

- Obvious solution

$$\mathbf{E}_a(t) = -g_{a\gamma} \mathbf{B}_e a(t)$$

ABRACADABRA (Proposed 2016)

PRL **117**, 141801 (2016)

- A Broadband/Resonant Approach to Cosmic Axion Detection with an Amplifying B-field Ring Apparatus
- Broadband approach
  - limited by SQUID noise (1/f noise below 50 Hz)
- Resonant approach
  - resonant freq. tuned with C
  - $Q=10^6$
  - feedback damping can be employed
  - limited by thermal noise of pickup loop

broadband

resonant

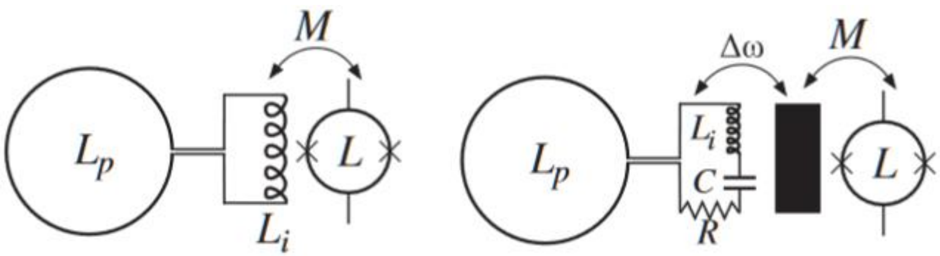

FIG. 3. Schematics of our readout circuits. Left: broadband (untuned magnetometer). The pickup loop L_p is placed in the toroid hole as in Fig. 1 and connected in series with an input coil L_i, which has mutual inductance M with the SQUID of self-inductance L. Right: resonant (tuned magnetometer). L_p is now in series with both L_i and a tunable capacitor C. A "black box" feedback circuit modulates the bandwidth $\Delta\omega$ and has mutual inductance M with the SQUID.

ABRACADABRA (Proposed 2016)

PRL **117**, 141801 (2016)

- Can reach QCD axion with GUT-scale decay constant
  $$f_a \sim 10^{16}\,\mathrm{GeV}$$
  $$m_a \sim 10^{-9}\,\mathrm{eV}$$
- 0.1 K, 1 yr measurement time (20 days per each resonant freq. for resonant approach)

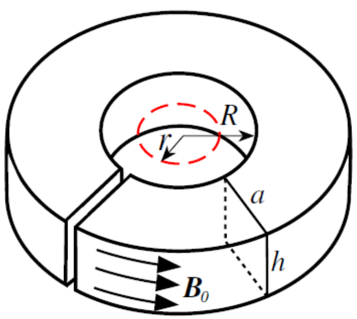

V_B = 1 m^3 when
r = R = a = h/3 = 0.85m

FIG. 1. A (gapped) toroidal geometry to generate a static magnetic field $\mathbf{B}_0$. The dashed red circle shows the location of the superconducting pickup loop of radius $r \leq R$. The gap ensures a return path for the Meissner screening current; see discussion in main text.

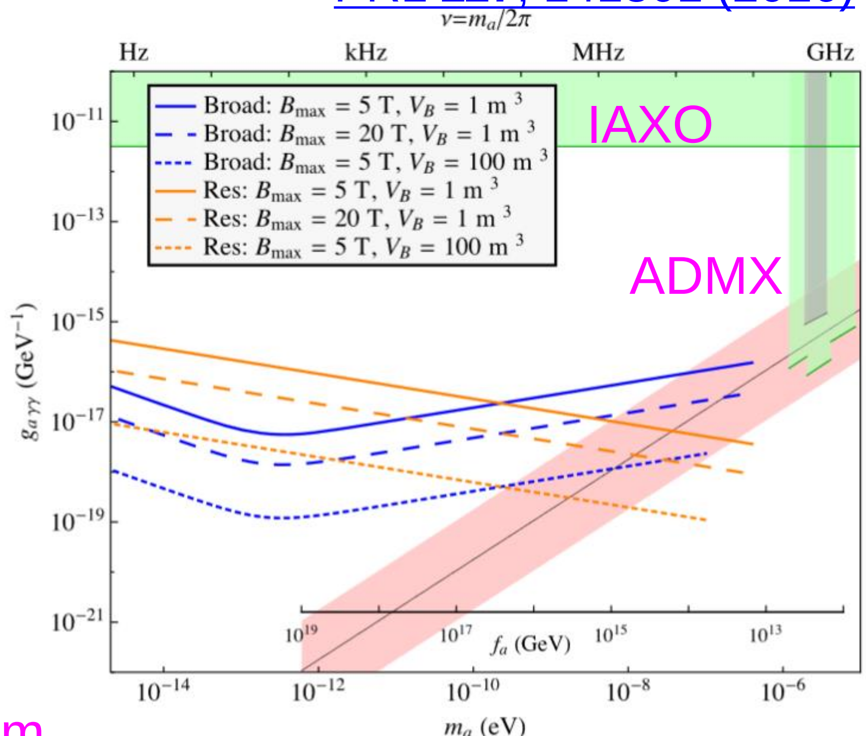

FIG. 2. Anticipated reach in the $g_{a\gamma\gamma}$ vs m_a plane for the broadband (Broad) and resonant (Res) strategies. The benchmark parameters are $T = 0.1$ K, $r = a = R = h/3$ (see Fig. 1), and $L_p = L_{\min} \approx \pi R^2/h$. The total measurement time for both strategies is $t = 1$ yr, where the resonant experiment scans from 1 Hz to 100 MHz. The expected parameters for the QCD axion are shown in shaded red, with the corresponding decay constant f_a inset at bottom right. The projected sensitivities of IAXO [41] and ADMX [14] are shown shaded in light green. Published limits from ADMX [13] are shown in gray.

ABRACADABRA-10cm (2018)

arXiv:1810.12257

- 1 T, Inner radius 3 cm, Outer radius 6 cm
- 1.2 K for toroid (870 mK for SQUID)
- Broadband approach
- 1 month of data
- Competitive to CAST limit
- First search for axion DM with $m_a < 1$ μeV

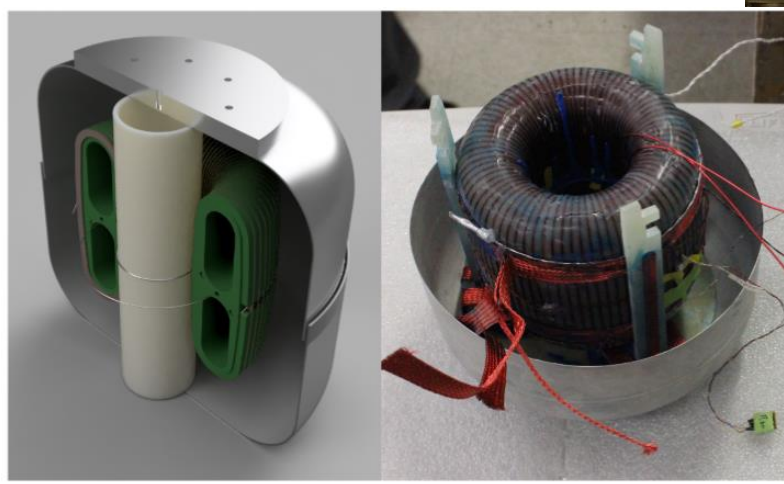

FIG. 1. *Left:* Rendering of the ABRACADABRA-10 cm setup. The primary magnetic field is driven by 1,280 superconducting windings around a POM support frame (*green*). The axion-induced field is measured by a superconducting pickup loop mounted on a PTFE support (white). A second superconducting loop runs through the volume of the magnet to produce a calibration signal. All of this is mounted inside a superconducting shield. *Right:* Picture of the exposed toroid during assembly.

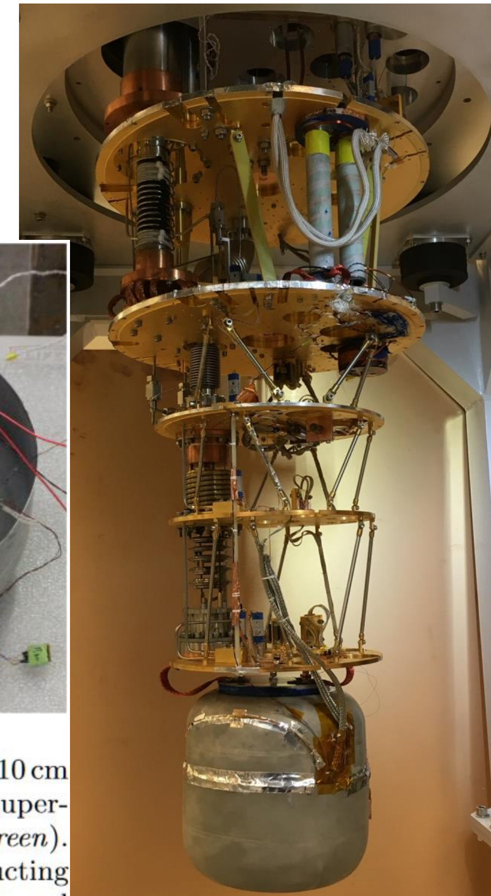

ABRACADABRA

http://abracadabra.mit.edu/

Bounds on Axion-Photon Coupling

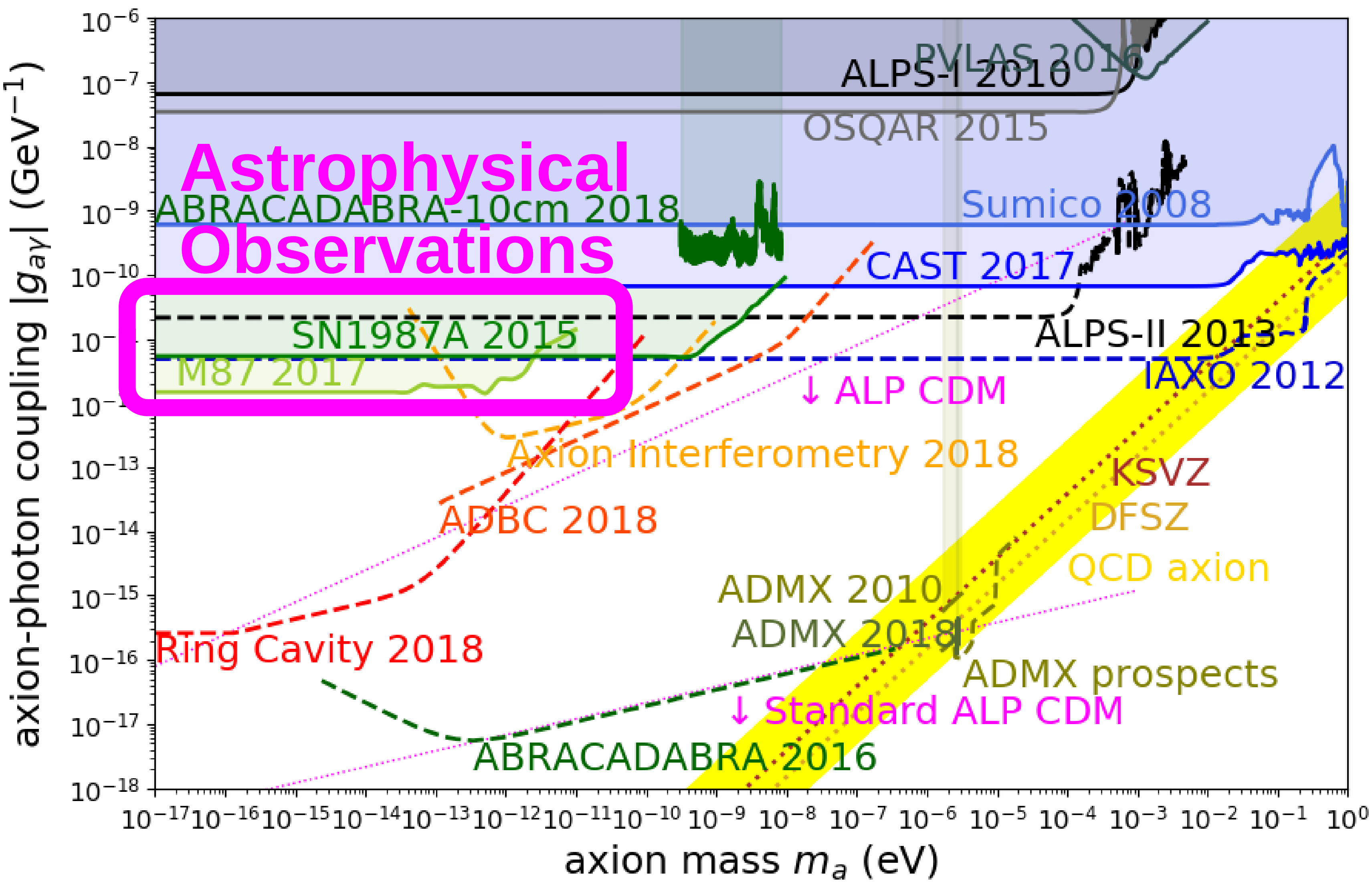

SN1987A (2015)

[JCAP **02**, 006 (2015)](JCAP 02, 006 (2015))

- Absence of gamma-ray signal from SN1987A
  - ALPs would be emitted from core-collapse supernova via Primakoff process
  - ALPs eventually convert into gamma-ray in the magnetic field of Milky Way (~ μG ~ 0.1 nT over ~ kpc)
- data from GRS (Gamma Ray Spectrometer) of SMM (Solar Maximum Mission) satellite coincidence with neutrino signal was used

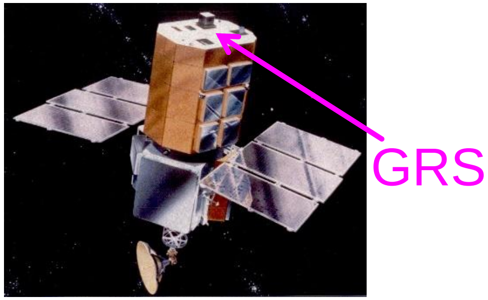

- Better limit possible by Fermi-LAT observation
- Dependent on supernova models and Milky Way magnetic field

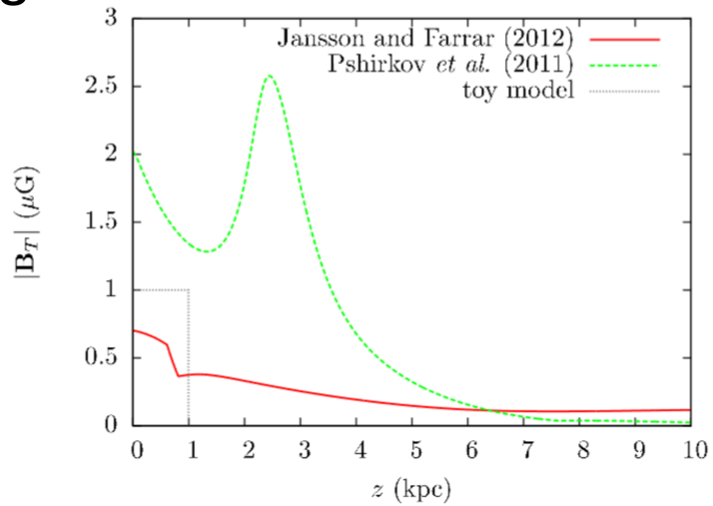

Figure 8. Norm of the transverse Galactic magnetic field as a function of the distance in the direction of SN1987A in various models.

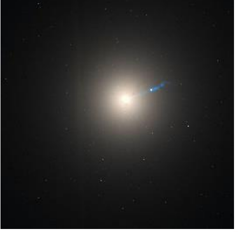

M87 (2017)

JCAP **12**, 036 (2017)

- Absence of substantial irregularities in the X-ray power law spectrum from M87 galaxy in Virgo cluster
  - close (16.4 Mpc) and hosts SMBH bright in X-ray
  - X-ray photon to ALPs conversion under magnetic field
  - magnetic field in Virgo (~35-40 μG) modeled from Faraday rotation measurements
    (magnetized plasma is birefringent and induces wavelength-dependent rotation of polarization of photons)
  - photon-ALP conversion probability is energy dependent and thus X-ray spectrum would change
- data from Chandra was used
- Dependent on Virgo magnetic field

Many Other Astrophysical Limits

Hydra A (58.3 Mpc) with Chandra (X-ray)
ApJ **772**, 44 (2013)

PKS 2155-304 (z=0.116)
with H.E.S.S. (γ-ray)
PRD **88**, 102003 (2013)

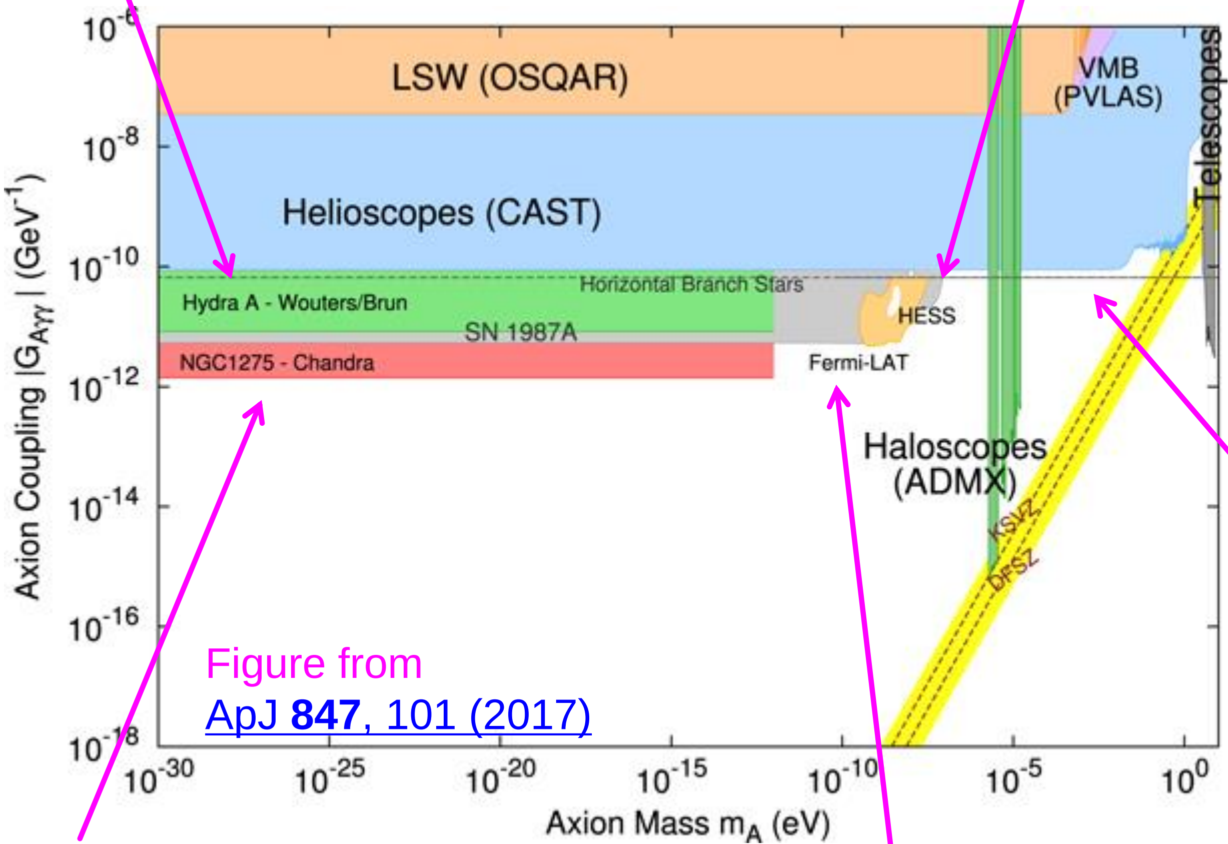

Figure from
ApJ **847**, 101 (2017)

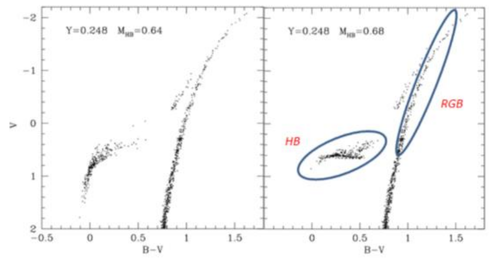

Ratio of horizontal branch stars to red giants in globular clusters (HB stars reduce with axion-photon coupling)
PRL **113**, 191302 (2014)

NGC1275 with Chandra (X-ray)
ApJ **847**, 101 (2017)

NGC1275 (68.2 Mpc) with Fermi-LAT (γ-ray)
PRL **116**, 161101 (2016)

Bounds on Axion-Photon Coupling

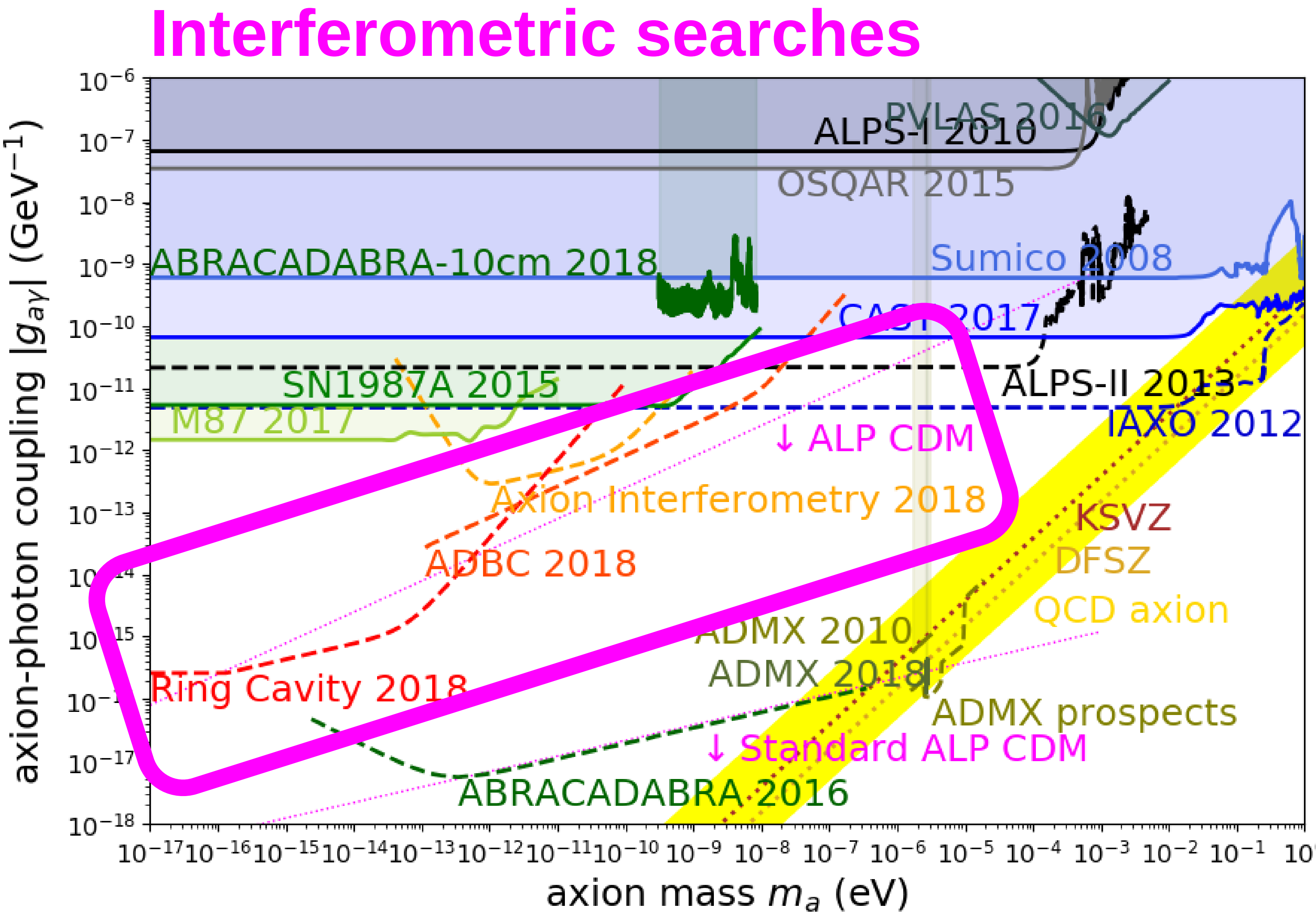

Interferometric Searches

- Light speed difference between two circular polarizations

$$c_\pm = \sqrt{1 \pm \frac{g_{a\gamma} a_0 m_a}{k} \sin(m_a t + \delta_\tau)}$$

Can be derived from Maxwell-Axion equations

- If local ALP density = local DM density, $\varrho_a = \frac{m_a^2 a_0^2}{2} = \varrho$

$$\delta c \equiv |c_+ - c_-|$$
$$\simeq 3 \times 10^{-24} \left(\frac{g_{a\gamma}}{10^{-12}\,\mathrm{GeV}} \right) \sin(m_a t + \delta_\tau)$$

local DM density (0.3 GeV/cm^3)

phase which changes with time scale

$$\tau = \frac{\lambda}{v} = \frac{2\pi}{m_a v^2}$$

de Broglie wavelength

axion velocity (assume dark matter velocity 10^{-3})

- Can be measured with laser interferometers and cavities
- Can be measured without magnets!
- Also assumes ALP = dark matter

Coherent Time Scale

- SNR grows with √Tobs if integration time is shorter than coherent time scale
- SNR grows with (Tobs)$^{1/4}$ if integration time is longer

$$\mathrm{SNR} = \begin{cases} \dfrac{\sqrt{T_{\mathrm{obs}}}}{2\sqrt{S_{\mathrm{noise}}(f)}}\dfrac{\delta c}{c} & (T_{\mathrm{obs}} \lesssim \tau) \\ \dfrac{(T_{\mathrm{obs}}\tau)^{1/4}}{2\sqrt{S_{\mathrm{noise}}(f)}}\dfrac{\delta c}{c} & (T_{\mathrm{obs}} \gtrsim \tau) \end{cases}$$

$$\tau \simeq 1\ \mathrm{year}\left(\frac{10^{-16}\ \mathrm{eV}}{m_a}\right)$$

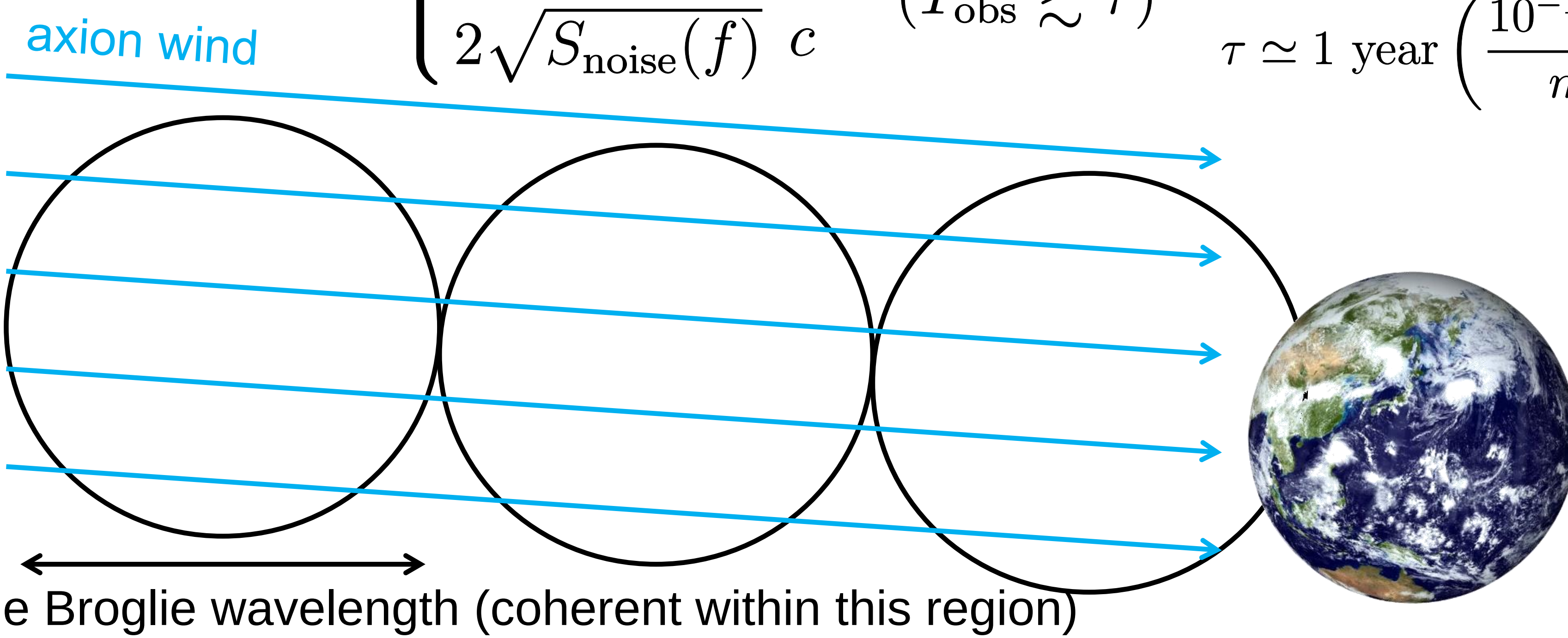

DeRocco + Hook (2018)

PRD **98**, 035021 (2018)

- Linear cavity with quarter wave plates inside
  mirror reflection flips left-handed to right-handed
- 40 m, finesse 10^6, intra cavity power 1 MW, 30 days integration

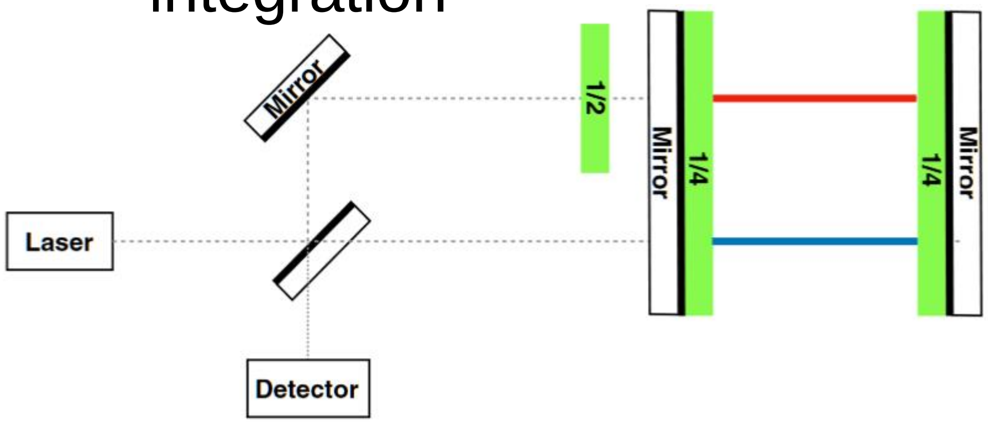

FIG. 3. A diagram of our proposed axion interferometer where the same mirrors are used to form both cavities. The dotted line is linearly polarized light, the red line is ↺ polarized light and the blue line is ↻ polarized light. Two quarter wave plates and a half wave plate are used to maintain the circular polarization of the light. This setup cancels the radiation pressure noise associated with the displacement of the mirror, leaving only noise due to radiation torque. Torque noise in this setup can be several orders of magnitude smaller than the radiation pressure noise experienced by the setup in Fig. 2.

radiation pressure torque noise at low freq.

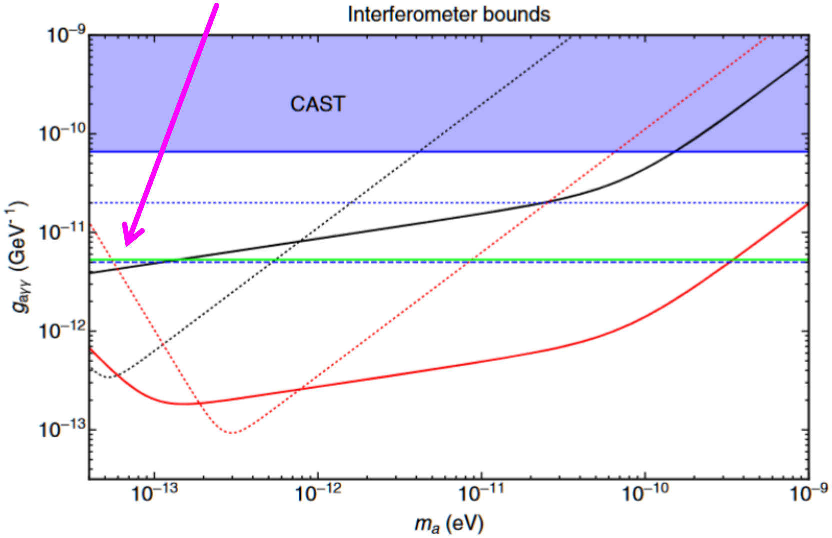

FIG. 5. Same as Fig. 4 but using the configuration shown in Fig. 3. Radiation pressure noise is cancelled leaving only radiation torque noise. We take the beams to be separated by 1 cm and the mirror to be circular and 10 cm in diameter.

Obata + Fujita + Michimura (2018)

[PRL **121**, 161301 (2018)](#)

- DARC: Dark matter Axion search with a Ring Cavity (tentative)
- Bow-tie configuration to keep polarization modes
- Double-pass for common mode rejection

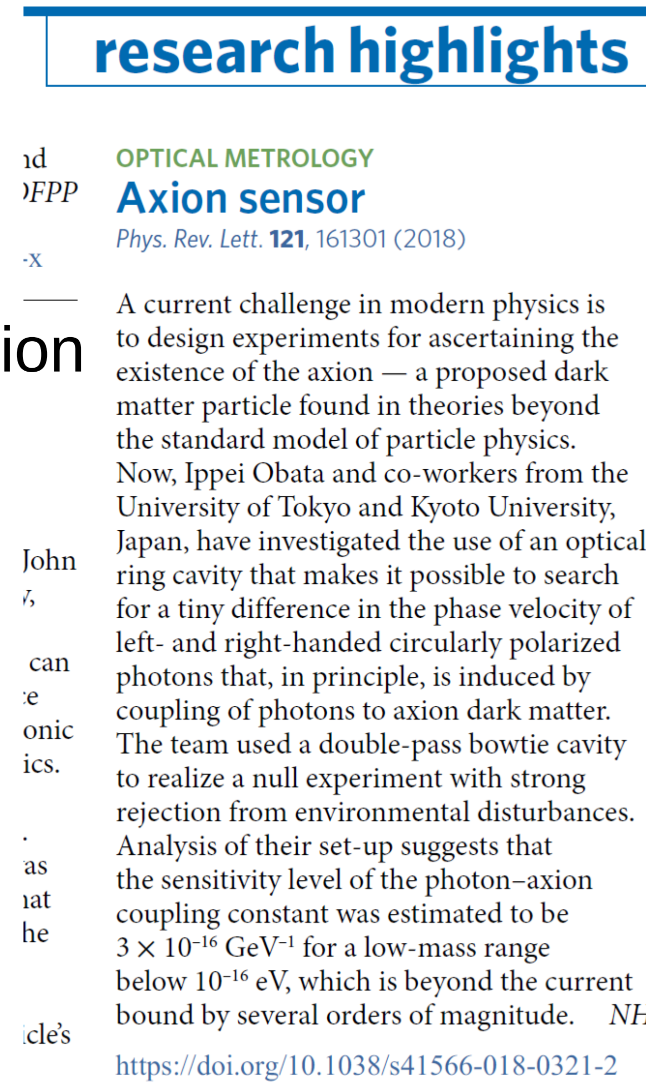

research highlights

OPTICAL METROLOGY

Axion sensor

Phys. Rev. Lett. **121**, 161301 (2018)

A current challenge in modern physics is to design experiments for ascertaining the existence of the axion — a proposed dark matter particle found in theories beyond the standard model of particle physics. Now, Ippei Obata and co-workers from the University of Tokyo and Kyoto University, Japan, have investigated the use of an optical ring cavity that makes it possible to search for a tiny difference in the phase velocity of left- and right-handed circularly polarized photons that, in principle, is induced by coupling of photons to axion dark matter. The team used a double-pass bowtie cavity to realize a null experiment with strong rejection from environmental disturbances. Analysis of their set-up suggests that the sensitivity level of the photon–axion coupling constant was estimated to be 3×10^{-16} GeV^{-1} for a low-mass range below 10^{-16} eV, which is beyond the current bound by several orders of magnitude. *NH*

https://doi.org/10.1038/s41566-018-0321-2

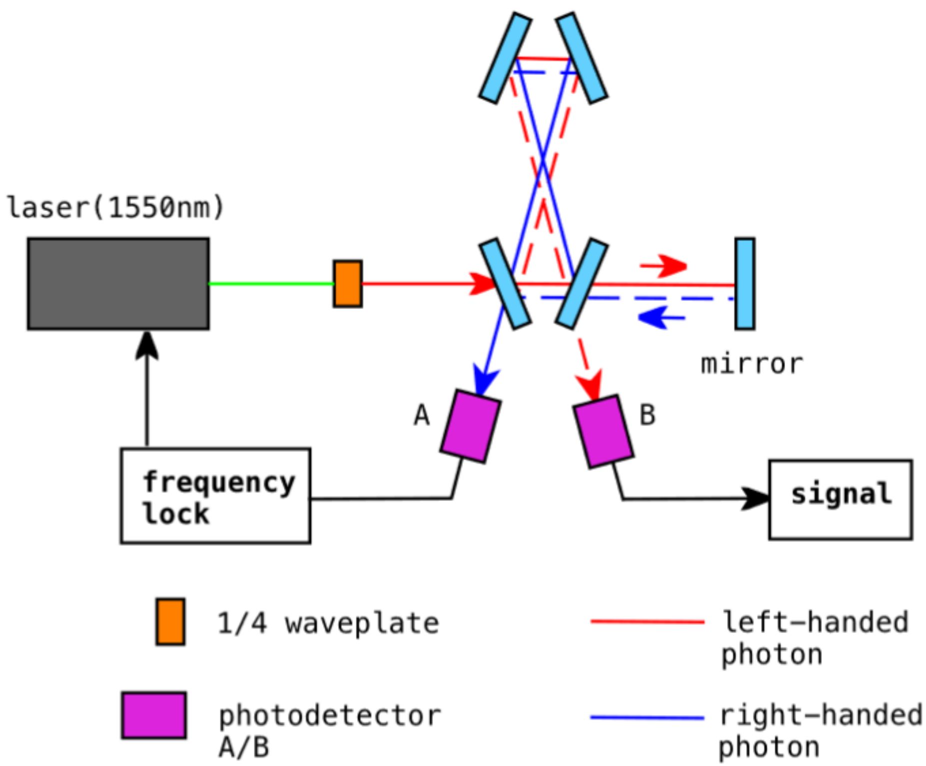

[Nature Photonics **12**, 719 (2018)](#)

Obata + Fujita + Michimura (2018)

- 10 m, finesse 10^6, 100 W input, 1 year integration
  - this means 30 MW intra cavity power
- Note that mirror complex reflectivity difference between p and s polarizations from nonzero incident angle was not considered (incident angle tuning necessary)

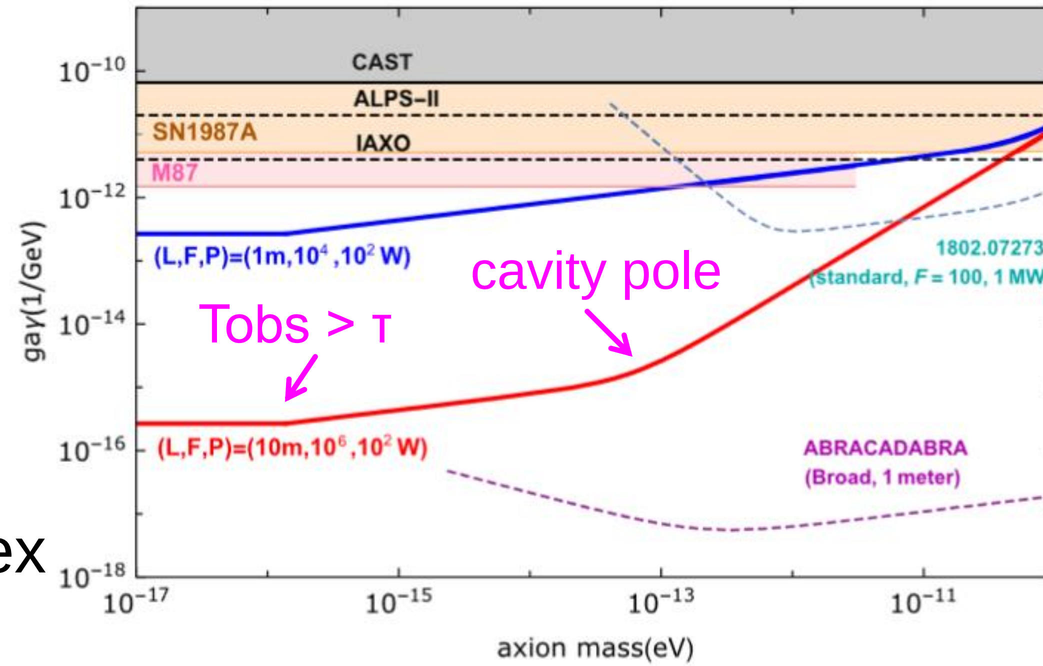

FIG. 2. The sensitivity curves for the axion-photon coupling constant $g_{a\gamma}$ with respect to the axion mass m. The solid blue (red) line shows the sensitivity of our experiment $(L, F, P) = (1(10)\ \mathrm{m}, 10^4(10^6), 10^2(10^2)\ \mathrm{W})$. The gray band represents the current limit from CAST [5]. The dashed black lines are the prospected limits of IAXO [6] and ALPS-II [7] missions. The dashed turquoise blue and purple lines show the proposed reaches of axion optical interferometer suggested in [10] and ABRACADABRA magnetometer [12]. The orange and pink bands denote the astrophysical constraints from the cosmic ray observations of SN1987A [15] and radio galaxy M87 [17].

ADBC by MIT Group (2018)

arXiv:1809.01656

- Axion Detection with Birefringent Cavities
- Use linear polarization and detect sidebands of other polarization

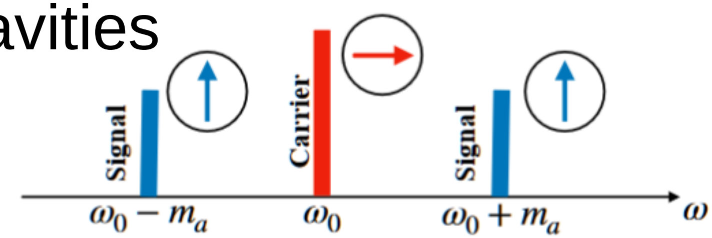

- Tune incident angle for resonant detection at high freqs.
- 40 m, finesse 2e5 for → (3e3 for ↑), intra cavity power 1 MW, 30 days integration in total

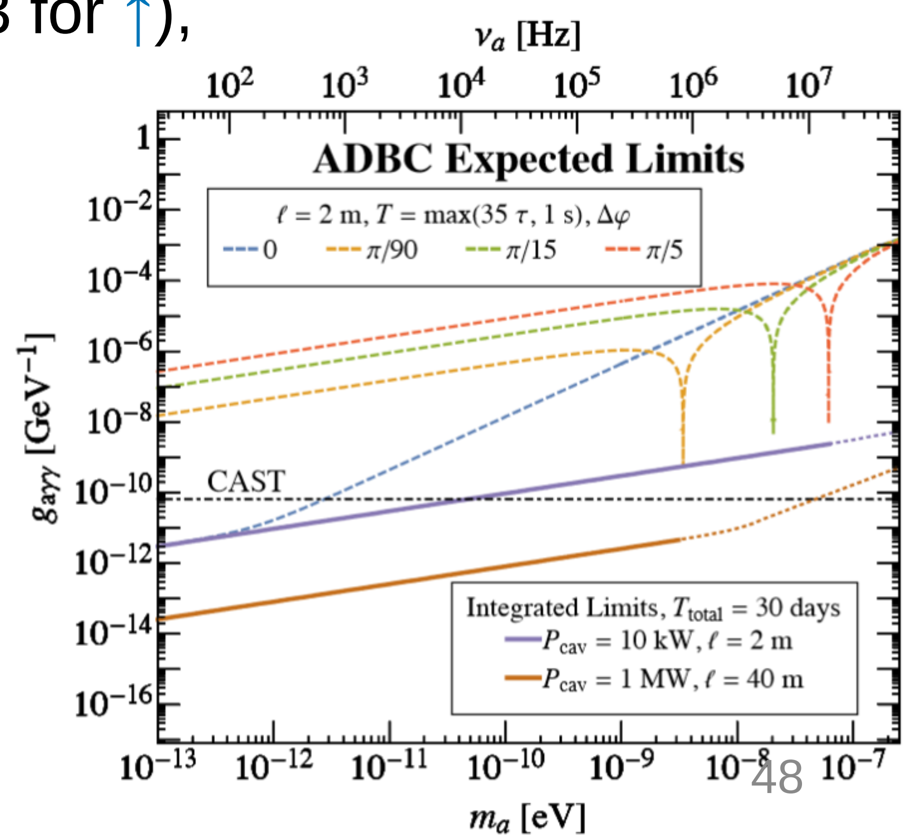

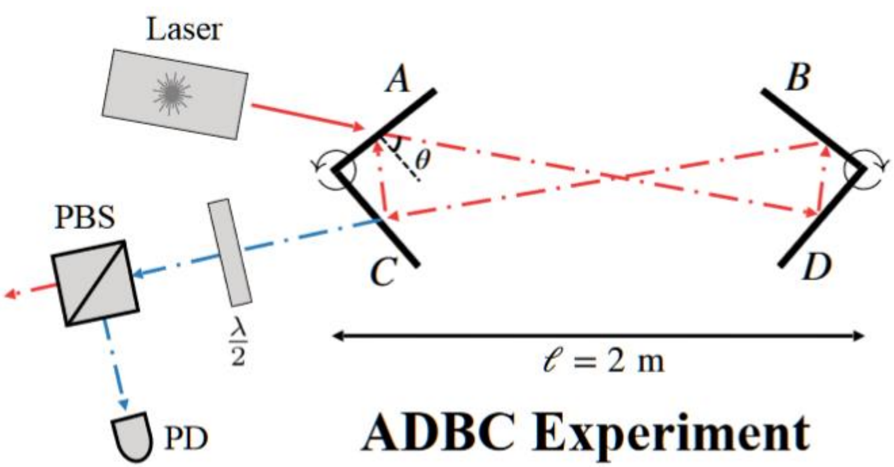

FIG. 2: Schematic of the ADBC experiment. The red optical

Sensitivity Design

- Brute force necessary, you cannot win for free

  NOTE that $\delta c \propto \lambda_{laser}$ and shot noise $\propto \sqrt{\lambda_{laser}}$

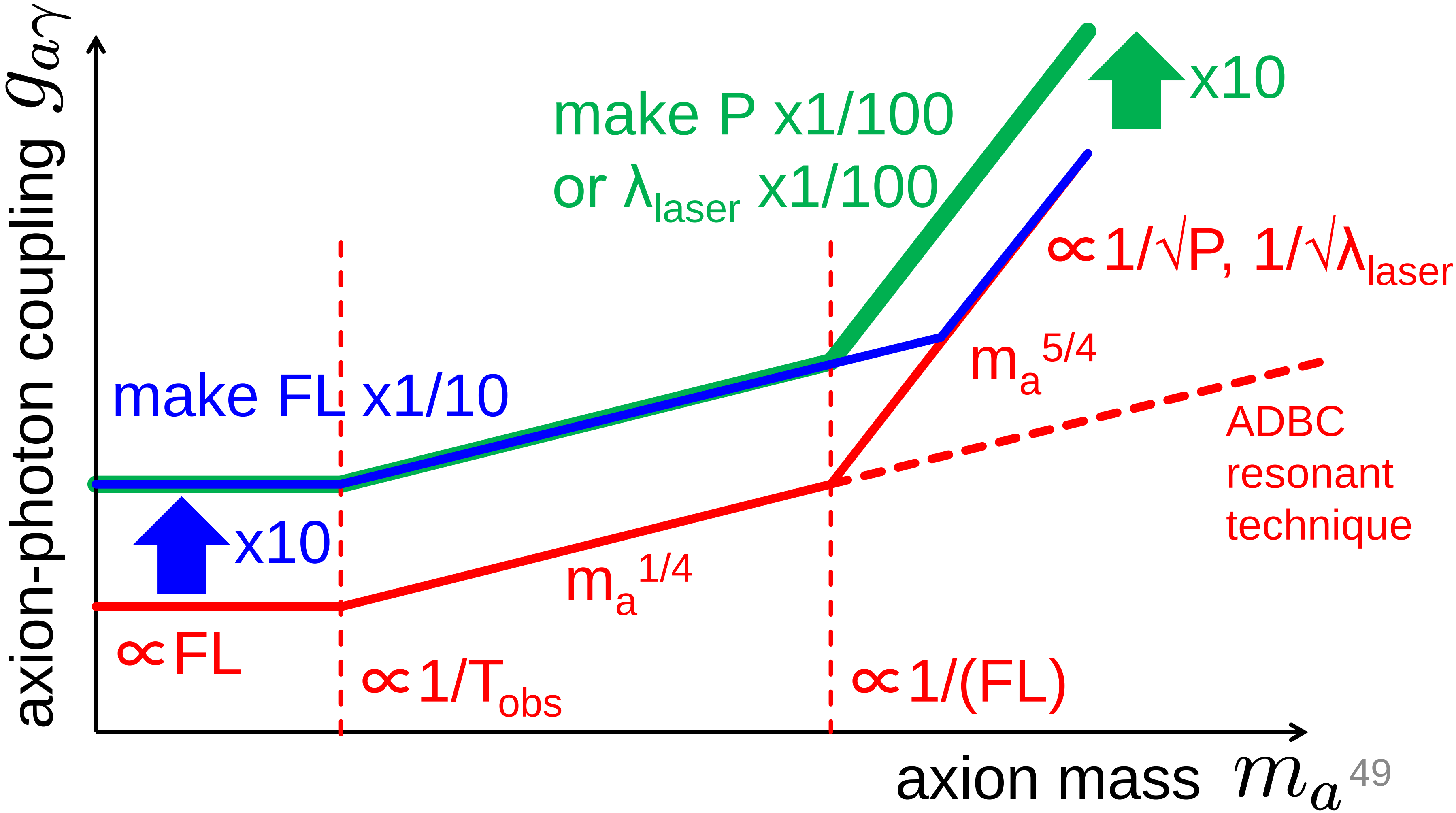

Prototype Experiment

- 1 m, finesse 10^4, 0.1 W input gives limit beyond CAST
- Assuming shot noise limited sensitivity of 6e-20 /rtHz (@ 0.01-100 Hz)

easy prototype
1e-15 /rtHz

"feasible" prototype

ultimate

ADBC broadband setup looks easiest to implement first

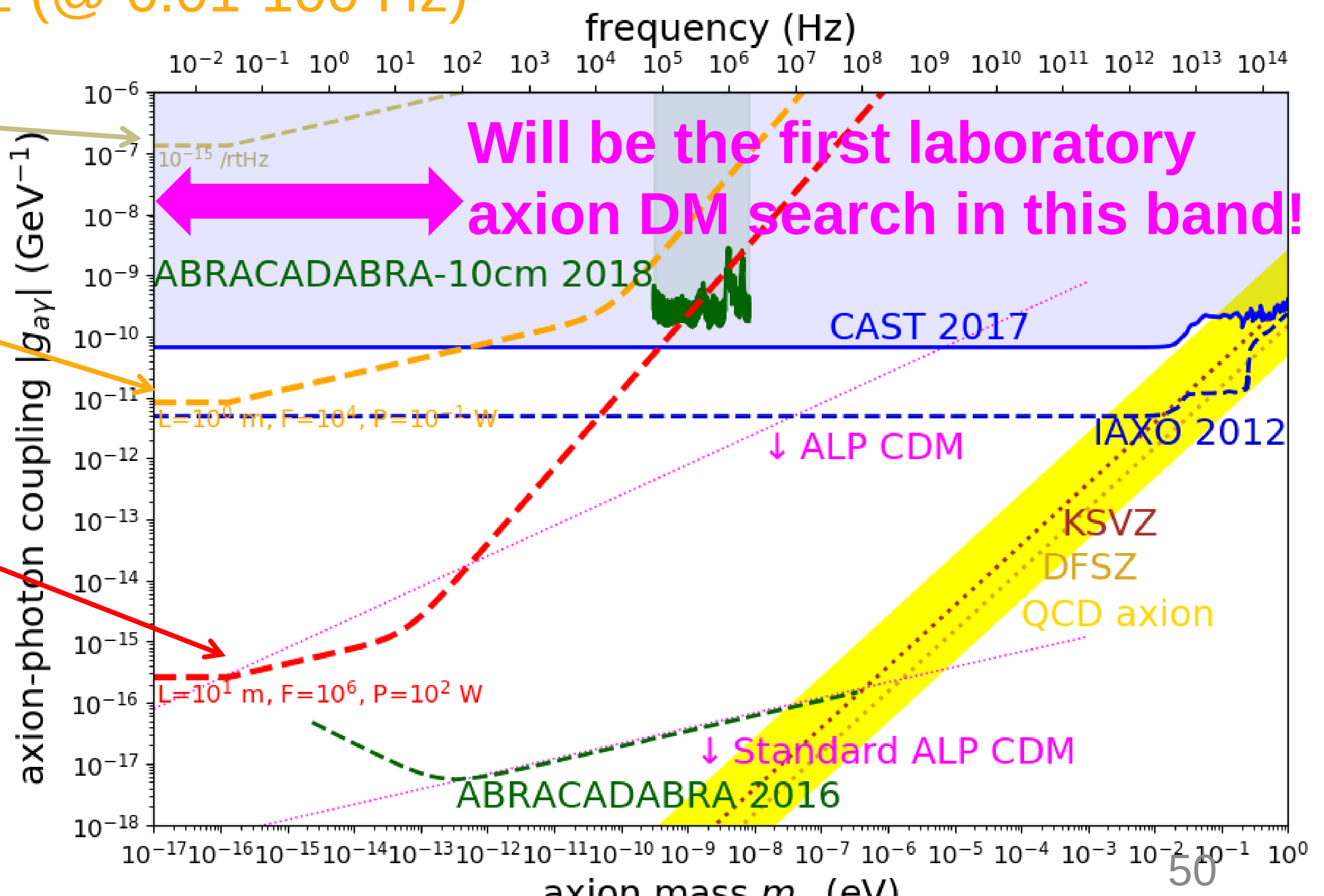

Comparison of Frequency Noise

- Sakai, Takada achieved ~10^{-13} /rtHz with double-pass ring cavity (stationary, with silicon)
- Ushiba achieved ~10^{-15} /rtHz with cryogenic silicon cavity (without double-pass CMRR)
- State-of-the-art at ~1e-16 (without double-pass CMRR)

http://granite.phys.s.u-tokyo.ac.jp/theses/takeda_m.pdf

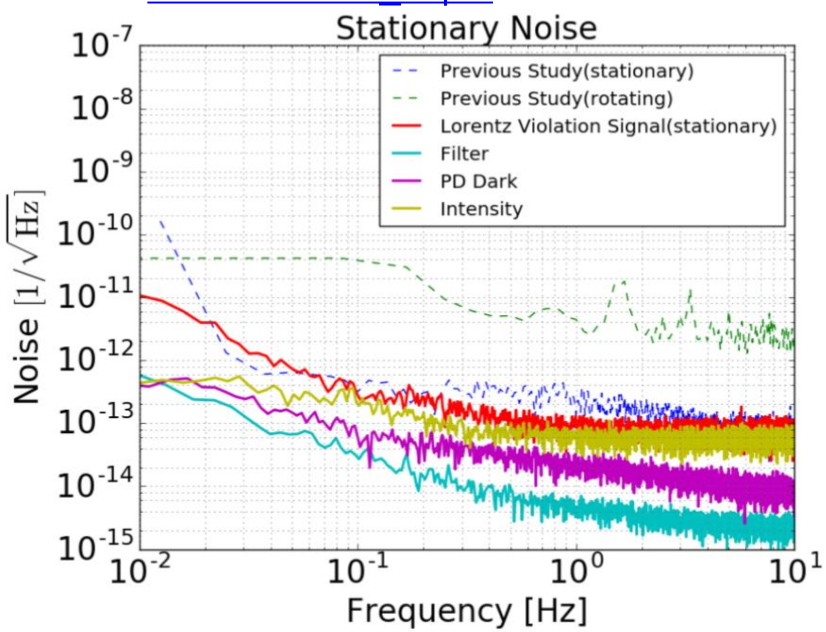

http://granite.phys.s.u-tokyo.ac.jp/theses/ushiba_thesis.pdf

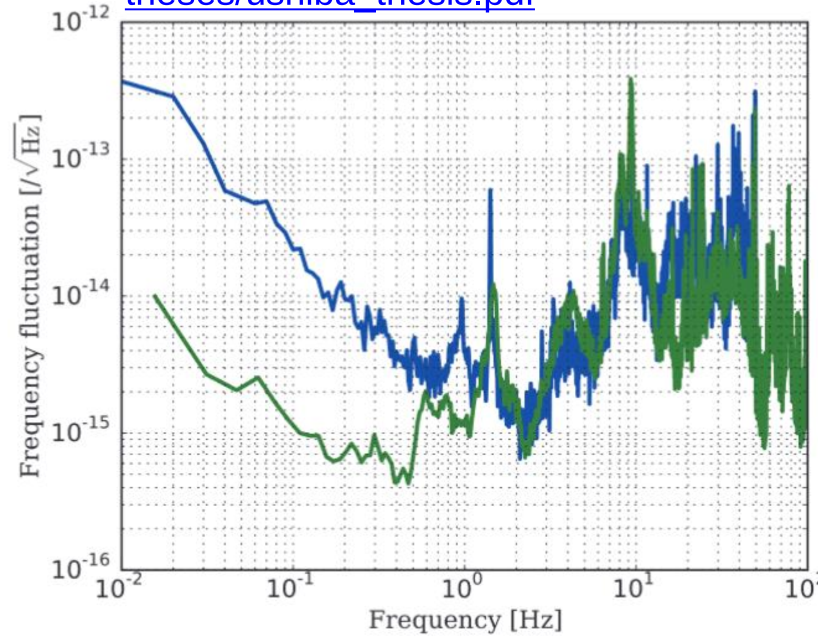

Some Other Ideas

- Somehow make an experimental set up which is not affected by the coherent time scale
- Signal extraction mirror to enhance bandwidth
- Nagano cavity
- Axion-graviton coupling?

Other Interesting Topics

- Axion hot dark matter bounds from CMB
  JCAP **08**, 001 (2010) (m_a<0.91 eV from WMAP)
  JCAP **02**, 003 (2011) (m_a<~0.7 eV from WMAP)
  JCAP **10**, 020 (2013) (m_a<0.67 eV from Planck and WMAP)
  Phys. Lett. B **752**, 182 (2016) (m_a<0.529 eV from Planck)
- ALP CDM models
  for example, JCAP **06**, 013 (2012)
- Bound from globular clusters (horizontal branch stars)
  PRL **113**, 191302 (2014)
- MADMAX (dielectric haloscopes)
  PRL **118**, 091801 (2017)
- Astrophysical polarization measurements
  T. Fujita+, arXiv:1811.03525
- A new era in the search for dark matter
  Nature 562, 51 (2018)

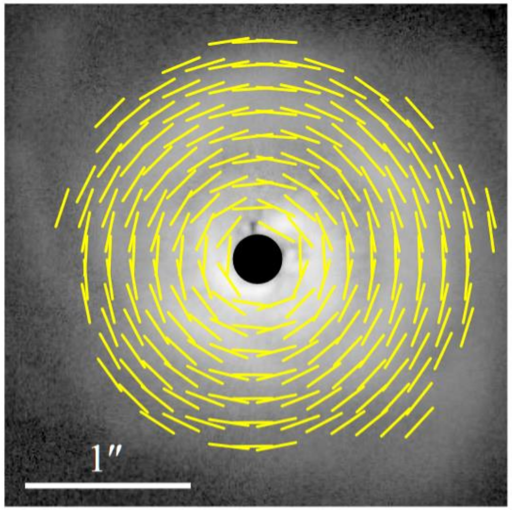

ApJL **729**, L17 (2011)

Summary

- Model independent searches
  - LSW (ALPS, OSQAR)
  - birefringence measurements (PVLAS)
- Solar axion searches (quite robust)
  - helioscopes (Sumico, CAST, IAXO)
- DM axion searches (assumes ALP density = DM density)
  - haloscopes (ADMX)
  - DM induced magnetic field detection (ABRACADABRA)
  - interferometric searches (DARC, ABDC)

    can be done without magnets!

- Axion search looks interesting than I had imagined
- Demonstration of DARC will be the first laboratory search for axion DM with $m_a < \sim 0.1$ neV